EFFECT OF TITANIUM PICK-UP ON MOULD FLUX VISCOSITY IN CONTINUOUS CASTING OF TITANIUM-STABILISED STAINLESS STEEL

By

Tshikele Mukongo

Dissertation submitted in partial fulfillment of the degree

Master of Engineering

in the

Department of Materials Science and Metallurgical Engineering,

Faculty of Engineering

at the

University of Pretoria

Supervisor: Prof. P.C. Pistorius

PRETORIA

2003

ABSTRACT

Title : Effect of titanium pick-up on mould flux viscosity in continuous casting of titanium-stabilised stainless steel
Author : Tshikele Mukongo
Supervisor : Prof. P.C. Pistorius
Department : Materials Science and Metallurgical Engineering
Degree : Master of Engineering

The behaviour of mould fluxes used in continuous casting of two Ti-stabilised stainless steels was investigated in terms of the level of titanium pick-up by the flux and the effect of this absorption of titanium on the viscosity of the fluxes.
The two fluxes considered are respectively used for the casting of a ferritic steel (type 409) and an austenitic steel (type 321).

Concerning the titanium pick-up (expressed as TiO_2), the TiO_2 content of the flux stabilised at about 3-4% for the mould flux of the ferritic steel and at about 6% for the mould flux of the austenitic steel after 20 minutes of casting. At the same time due to the reduction of SiO_2 in the molten flux by TiN and Ti in the steel the basicity of the mould flux of the ferritic steel increased from 0.8 to 0.9 while it increased from 0.95 to 1.2 for the mould flux of the austenitic steel.

The SEM/EDS analysis of the sampled flux during casting showed only some spherical metallic droplets in the case of the mould flux of the ferritic steel but for the mould flux of the austenitic steel apart from the metallic droplets, some precipitates rich in Ca, Ti and O were identified in the glassy phases.

Rotational viscometry carried out on the two fluxes showed that there is a decrease in the viscosity of the fluxes with the absorption of TiO_2, Ti_2O_3 and Ti_3O_5 in the range of 2 to 10 wt%, for temperatures from 1400°C to 1200°C.

The effect of TiO_2 and Ti_2O_3 has been tested with the mould flux of the austenitic steel at a basicity of 1.2 to match the basicity which arises during casting. For temperatures of 1250°C and below, the apparent viscosity of the flux increased markedly with the absorption of 10 % of TiO_2 or Ti_2O_3. In both cases precipitation of perovskite ($Ca_2Ti_2O_6$ or $Ca_2Ti_2O_5$) was found to be responsible for the increase of the apparent viscosity of the flux of the austenitic steel.

Keywords: continuous casting, titanium-stabilised stainless steels, ferritic steel, austenitic steel, titanium nitride, viscosity, mould flux, basicity, perovskite, lubrication.

ACKNOWLEDGEMENTS

I wish to thank gratefully:

- Prof. P.C. PISTORIUS, for identifying the project, valuable advice, guidance and supervision.
- The personnel of Columbus Stainless, and especially WILLEM ORBAN and JOHAN ACKERMANN, for much help with obtaining mould flux samples, and financial support.
- The Technology and Human Resources for Industry Programme of the Department of Trade and Industry of South Africa, and the National Research Foundation for financial support.
- LILIE TSHIKELE, for your unconditional support during the project.
- All friends, for your support and encouragement during the project.

TABLE OF CONTENTS

1. INTRODUCTION

Mould fluxes are synthetic slags routinely used during the continuous casting of steel. It is well known that the performance of the fluxes can greatly affect caster operations in terms of both operation and product quality. The major functions of mould fluxes are the thermal insulation of the liquid steel, protection of the molten steel against oxidation, absorption of non-metallic inclusions, lubrication of the gap between the mould wall and the solidified steel and promotion of homogeneous heat transfer between the strand and the mould. All these functions are essential and an inadequacy in one of them can result in serious defects and inferior steel surface quality.

During the continuous casting process there can be a change in the chemical composition and physical properties (viscosity and crystallisation temperature) of the mould flux owing to the reactions at the steel-slag interface (including the absorption of non-metallic inclusions rising from the steel).

For Ti-stabilised stainless steel, TiN precipitation appears inevitable during continuous casting. The precipitation of this solid material during processing can cause nozzle clogging, sticking in the mould, surface defects on the surface of the casting and can also affect the lubrication properties of the mould flux [Sharan et al, 1995].

Ti dissolved in steel can also reduce silica in the slag to form some titanium oxides.
All those titanium compounds, when picked up by the molten flux, can modify its characteristics (viscosity and crystallisation behaviour) and thus its lubrication and heat transfer characteristics.

It is then important to understand the chemistry of formation of titanium compounds during continuous casting of Ti-stabilised stainless steel and their effect on the performance of mould fluxes.
The objective of this study is to investigate the behaviour of two mould fluxes used in continuous casting of a ferritic (type 409) and an austenitic (type 321) Ti-stabilised

stainless steel in terms of the level of Ti pick-up, and the effect of Ti pick-up on the viscosity of the two fluxes.

2. LITERATURE SURVEY

2.1. Ti behaviour during continuous casting of Ti-stabilised stainless

2.1.1. Formation of non metallic inclusions

2.1.1.1. Origin of the inclusions

Most of the casting difficulties or surface defects with Ti-stabilised grades which manifest themselves at the caster and in the final product, essentially result from the formation of various solubility product inclusions such as Al_2O_3 (when Al is added to the steel as deoxidant), TiN or Ti_3O_5. These inclusions normally start to form in the ladle following Al or Ti additions, and continue to precipitate as the steel cools. They may or may not react with other inclusions arising from slag entrapment during tapping, or with other large exogenous inclusions such as refractories. Such inclusions can lead to several phenomena in the ladle, tundish and mould, such as mould lumps (floaters) and clogging, and can finally result in line or skin lamination defects in the slab and rolled strip after casting.[Nunnington and Sutcliffe, 2002]

The main solid inclusion of interest in Ti-stabilised stainless steel is TiN especially when steel is not fully Al-killed. TiN is formed from titanium and nitrogen dissolved in steel.

The titanium is sometimes added intentionally (in the case of the titanium stabilised grade), or it may originate from the raw materials used in manufacturing the stainless steel. Nitrogen is generally picked up from the atmosphere during steelmaking, and may also be intentionally added as an alloying element. Typical compositions of two titanium stabilised stainless steels are given in the Tables 2.1 and 2.2 below:

Table 2.1: *Typical composition of Ti-stabilised stainless steel type 321 [Orban, 2003]*

C	Cr	Ni	Mo	Mn	Ti	N	Si	Cu	S	Al	Nb	O
0.034	17.2	9.14	0.12	1.17	0.309	0.014	0.46	0.013	0.004	0.009	0.002	0.002

Table 2.2: *Typical Composition of Ti-stabilised stainless steel type 409 [Orban, 2003]*

C	Cr	Ni	Mo	Mn	Ti	N	Si	Cu	S	Al	Nb	O
0.009	11.62	0.13	0.01	0.36	0.184	0.011	0.56	0.14	0.001	0.004	0.002	0.006

Type 409 stainless steel is a "ferritic" stainless steel, whereas type 321 is an "austenitic" stainless steel.

In general titanium stabilised stainless steels can contain up to 0.75 % of Ti and 0.1% of N.

Titanium reacts with this nitrogen dissolved in the liquid steel to form solid titanium nitride in the mould of the continuous caster where the temperature of the steel drops to the liquidus temperature.

The role of TiN in casting problems and surface defects is shown schematically for mould area in Figure 2.1 [Nunnington and Sutcliffe, 2002]

These include the solidified δ- ferrite clog stabilised with TiN network, mould lumps (floaters) and clusters of TiN which have reacted with the mould flux and become entrapped at the strand surface

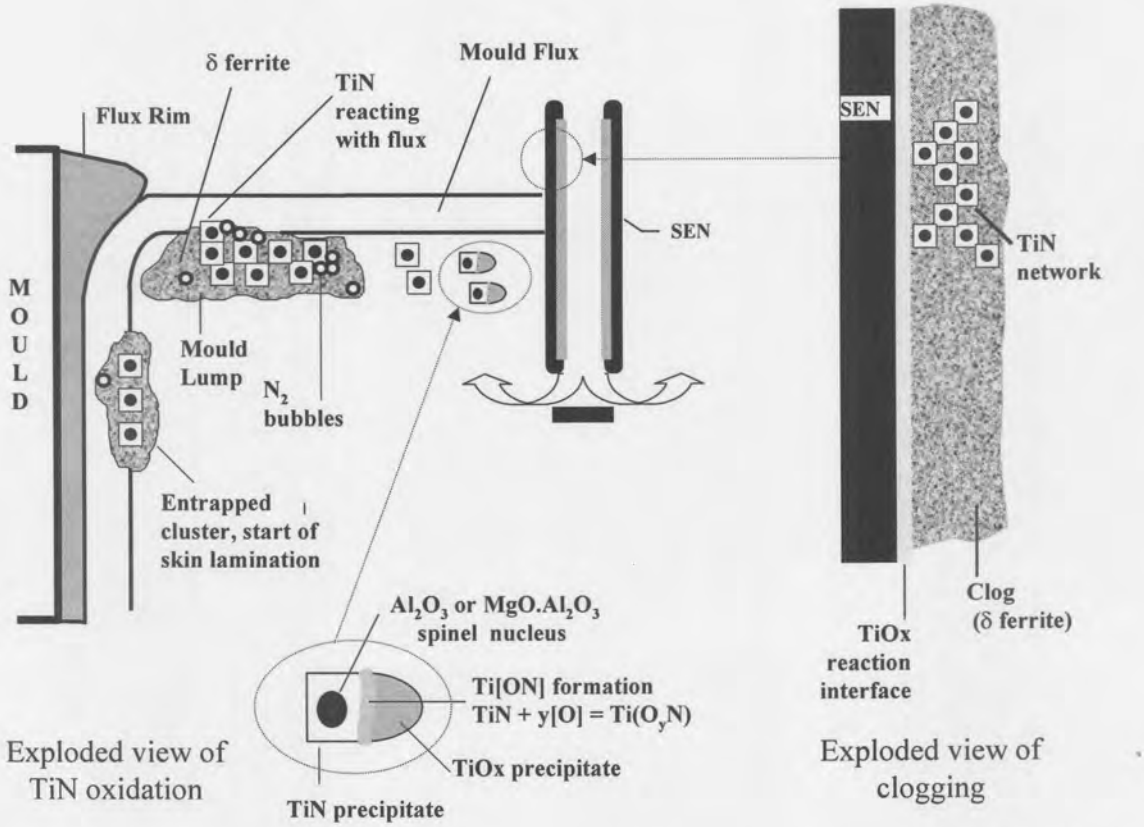

Figure 2.1: *Schematic of the caster and associated casting problems associated with TiN formation in the steel [Nunnington and Sutcliffe, 2002].*

It is then important to understand the chemistry of the formation titanium nitride in liquid steel in order to predict the conditions under which it will form.

2.1.1.2 Thermodynamic considerations

The thermodynamics of the precipitation of inclusions in titanium treated steels has been discussed by many authors.[Turkdogan, 1990; Liao et al, 1990; Ozturk et al, 1995].

All of them determined the equilibrium conditions for titanium nitride formation in steels containing titanium and nitrogen. The formation of solid titanium nitride from dissolved nitrogen and titanium can be represented by the following equilibrium reaction:

$$[Ti] + [N] = TiN_{(s)} \quad (2.1)$$

$$\Delta G^o = -73\,840 + 27.33\ T \text{ cal/mole} \quad \text{[Turkdogan, 1990]} \quad (2.2)$$

There are others relationships for the calculation of this ΔG^o in the literature.

The following sources can be quoted:

- From data compiled by Pehlke [1973] :

$$\Delta G^o = -67\,760 + 27.2\ T \text{ cal/mol} \quad (2.3)$$

- From data compiled by the Japan Society for the Promotion of Science [1988]:

$$\Delta G^o = -\ 90732 + 35.67\ T \text{ cal/mol} \quad (2.4)$$

The values calculated from data compiled by Pehlke are closer to those compiled by Turkdogan than data from the Japan Society.

The equilibrium constant (K) for this reaction is given by:

$$K = \frac{a_{TiN}}{h_{Ti} \cdot h_N} = \frac{a_{TiN}}{f_{Ti}[\%Ti] \cdot f_N[\%N]} \quad (2.5)$$

where a=Raoultian activity, h= Henrian activity and f=Henrian activity coefficient.

Rearranging the above equation yields:

$$[\%Ti].[\%N] = \frac{a_{TiN}}{K.f_{Ti}.f_N} \quad (2.6)$$

When pure TiN precipitates, its Raoultian activity is one. This means that the conditions for precipitation are controlled by Henrian activities of titanium and nitrogen. These are affected by mass percentages in solution, and their activity coefficients. These activity coefficients depend strongly on the presence of other alloying elements in solution (and stainless steels by their nature contain high concentrations of alloying elements).

By means of the two activity coefficients f_{Ti} and f_N, one can calculate the product [%Ti]* [%N] in order to calculate the stability diagram of TiN.

For the two stainless steels mentioned before these activity coefficients were calculated by using the known thermodynamics and the following relationship:

$$\log f_i = \sum e_i^j [\%j] + \sum r_i^j [\%j]^2 \qquad (2.7)$$

Where e_i^j and r_i^j are respectively the first and second order interaction parameters of species j with specie i, which can be titanium or nitrogen. The values of e_{Ti}^j and e_N^j used for the calculation of f_{Ti} and f_N are given in the table below:

Table 2.3: *Values of interactions parameters e_{Ti}^j and e_N^j*

$i \cdot \cdot j$	C	Cr	Ni	Mo	Mn	Ti	N	Si	Cu	S	Al	O
Ti	-.64	.024	.011	-	-.043	.048	-2.10	.07	-	-.06	.004	-3.4
Sources	[4]	[30]	[4]		[30]	[40]	[30]	[4]		[4]	[40]	[40]
N	.13	-.045	.006	-.011	-.024	-.63	0.0	.047	.009	.013	.01	-0.12
Sources	[4,43]	[4,43]	[32]	[4,43]	[43]	[4,43]	[43]	[43]	[4,43]	[4,43]	[43]	[4,43]

The values of r_i^j are comparatively small and can be taken equal to 0.

From these values of e_{Ti}^j and e_N^j, f_{Ti} and f_N have calculated for the two steels grade 321 and 409.

For the type 321 theses values of f_{Ti} and f_N were calculated to be respectively 2.849 and 0.145 whereas for the type 409 the same values were 1.811 and 0.257.

The calculation of the product [%Ti][%N] needs also the equilibrium constant for some relevant temperatures. As said before, the most severe precipitation problems are found in the mould of the continuous caster, where the temperature is approximately equal to the liquidus temperature of the steel.

The values of the liquidus temperature were estimated by using the correlation of Schurmann et al [1997] for the typical compositions of the two Ti-stabilised steels with compositions given in the Tables 2.1 and 2.2.

For type 321, the calculated value is T_{liq} = 1455°C and for type 409 T_{liq}= 1501°C.

And the solubility product for TiN in each of these two steels at their liquidus temperature is therefore given below:

$[\%Ti]\,[\%N] = 0.001042$ for type 321 (2.8)

$[\%Ti]\,[\%N] = 0.00165$ for type 409 (2.9)

From these equations the stability diagram of TiN was constructed as shown below:

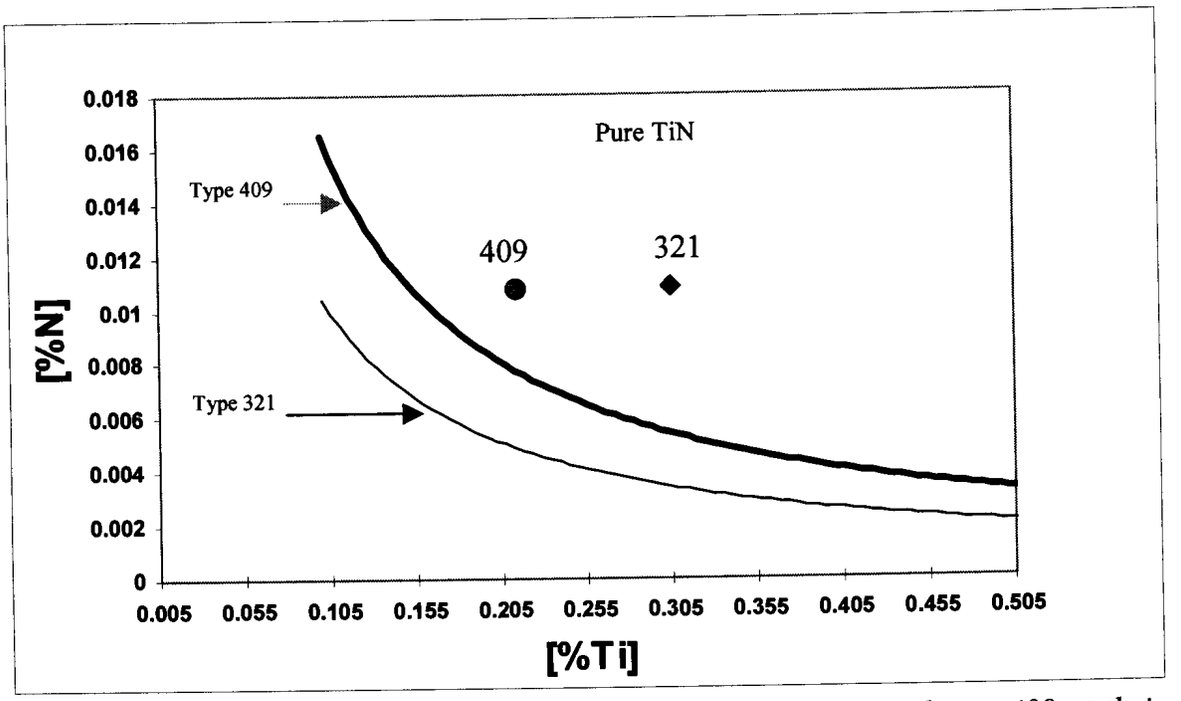

Figure 2.2: *Stability diagram for TiN in stainless steels type 321 and type 409 at their respective liquidus temperature,* ● *and* ♦ *are respectively the actual compositions for the two steels 409 and 321*

With such a diagram, the possibility of formation of TiN can be predicted for a certain temperature. Above the stability line precipitation of TiN can be expected.

It is clear that for both steels, the solubility product of titanium nitride is exceeded at the liquidus temperature as shown in the Figure above where the actual Ti and N contents of the two steels are represented; however the extent of supersaturation is greater for the austenitic steel, largely because its liquidus temperature is substantially lower (around 1450°C) than that of the ferritic steel (which has a liquidus temperature around 1500°C)

and its higher titanium content. As said before the precipitated TiN could cause nozzle clogging, sticking in the mould and surface defects during continuous casting [Liao & Fruehan, 1990].

It has been found practically that clogging is more prevalent with the ferritic grades than austenitic grades, as a result of the steel chemistry, particularly the lower solubility of [N] and [O], together with the higher liquidus and casting temperatures. In contrast to the ferritic grades, the austenitic grades tend to suffer less from clogging but more from mould lumps and surface defects. The reason of this behaviour is because of the lower liquidus and higher solubilities of [N] and [O], which result in the precipitation of solubility products at lower temperatures in the mould, rather than in the tundish and the SEN. Higher Ti levels in the austenitics can lead to severe lump formation, even curtailing casting, if any air ingress occurs as the steel is transferred from the tundish to mould [Nunnington and Sutcliffe, 2002].

2.1.2. Inclusion separation

The following criteria are necessary for optimized solid inclusion removal at the slag-metal interface during casting:

- flow patterns which maximize the rate of inclusion transport to an interface.
- A high contact angle between the inclusion and the liquid steel
- A slag covering which is designed to dissolve or wet the inclusion.

The removal of alumina based inclusions is well understood from an interfacial point of view, as there is a high contact angle (≈130deg) between alumina and liquid steel and the mould slags wet and dissolve alumina [Sharan et al, 1995].

Sharan et al [1995] conducted a few experiments aiming to determine the contact angles between liquid steel and a liquid slag sitting on a titanium nitride substrate. Their measurements indicated that the contact angle between a liquid iron, iron – 5percent Ni and 18 percent Cr – 8 percent Ni stainless steel in contact with calcium-aluminate slag and a TiN substrate was about 160 deg at 1550°C and when a liquid $CaO\text{-}Al_2O_3\text{-}SiO_2$

(30:10:60) slag was coexisting, the contact angle was 170 deg. This indicates that titanium nitride should almost emerge completely from a slag covered interface.

2.1.3. Dissolution of titanium nitride into slags.

Most mould slags are developed to dissolve alumina quickly and the absorption of alumina into the slags is generally not problematical; however the chemical behaviour of titanium nitride is not understood clearly [Sharan et al, 1995].

The strong wetting of titanium nitride by the lime-alumina-silicate slags suggests that the titanium nitrides will separate at the slag-metal interface and be absorbed by the mould flux; however, little is known concerning the solubility of titanium nitride in slags.

In some experiments conducted by Ozturk [1991] the solubility of titanium nitride based inclusions in some common ladle, tundish, mould fluxes was measured. A slag -nitride equilibration technique was used to determine the solubility of titanium nitride in different slags. For the nitride-slag equilibration, a recristallised alumina tube with gas tight seals at both ends was used in a carbon resistance furnace. The slag and nitride were placed in an alumina or molybdenum crucible. The crucible, with its contents, was suspended in the hot zone of the furnace. After the desired reaction time, the sample was quenched and prepared for chemical analysis. Table 2.4 gives experimental results obtained in these experiments.

Table 2.4: *Nitride solubility in Slags at T=1873K [Ozturk,1991]*

Slag	Nitride	%TiN
41% CaO-59%Al_2O_3	TiN	0.30wt%
36%CaO-54%Al_2O_3-10%SiO_2	TiN	0.332wt%
31%CaO-49%Al_2O_3-20%SiO_2	TiN	0.45wt%
Tundish flux	TiN	0.37wt%
Mould flux	TiN	0.45wt%

The solubility of TiN, as measured by Ozturk in calcium aluminates, a tundish flux and a mould flux, is less than 0.5 wt percent in all cases.

Mould flux and tundish flux chemistries are given in Table 2.5.

Table 2.5: *Compositions of the Mould and Tundish Fluxes used in the Experiments [Ozturk, 1991].*

Oxide	Tundish Flux	Mould Flux
CaO	40.2	37.85
Al_2O_3	29.45	2.35
SiO_2	8.5	45.11
MgO	0.60	1.82
TiO_2	7.25	8.66
MnO	-	4.19

Thus, for any appreciable concentration of TiN in the liquid steel, the mould or tundish flux will become saturated quickly with respect of TiN, leading to a two phase slurry of liquid flux and solid TiN. The result would be an increased viscosity of the mould flux due to solid precipitates of TiN. Solid precipitates or suspended matter in general are increasing the viscosity slightly when in low concentrations. High concentrations of suspended matter can cause substantial increases because of entanglement of the liquid between the particles [Bourne, 1982].

Actually titanium nitride formed in liquid steel was found to react with various slags and liberate nitrogen gas which nucleates at the titanium nitride-slag interface and causes bubbles within the liquid slag phase [Riquier et al, 1997].
Lindh [1997], proposes a few reactions, which can occur between mould slag and steel

$$TiN_{(s)} + (SiO_2) = (TiO_2) + 1/2\,(N_2)_{(g)} + [Si] \quad (2.10)$$

$$\Delta G^o = 49\,255 - 29.12\,T \text{ cal/mol} \quad (2.11)$$

$$3\ TiN_{(s)} + 5/2\ (SiO_2) = (Ti_3O_5) + 3/2\ (N_2)_{(g)} + [Si] \quad (2.12)$$

$$\Delta G^o = 155\ 463.8 - 100.87\ T\ cal/mol \quad (2.13)$$

Dissolved titanium can also reduce silica; therefore, titanium containing steels will react with high silica containing slags, such as mould and tundish slags, forming titania, which will dissolve within the mould [Sharan et al, 1995; Bommaraju, 1991].

$$[Ti] + (SiO_2) = (TiO_2) + [Si] \quad (2.14)$$

$$\Delta G^o = -22400 - 1.34\ T\ cal/mol\ [Pehlke, 1973] \quad (2.15)$$

$$[Ti] + 5/6\ (SiO_2) = 1/3\ (Ti_3O_5) + 5/6\ [Si] \quad (2.16)$$

$$\Delta G^o = -16027.5 - 1.2\ T\ cal/mol\ [Pehlke, 1973] \quad (2.17)$$

The above reactions show that the activity of SiO_2 in the slag is important in determining both Ti recovery and the formation of solubility products other than from [O] dissolved in the steel. The activity of SiO_2 in a typical mould flux for austenitic steel type 321 of composition (38 % SiO_2, 36.2 % CaO, 6.3 % Al_2O_3, 8.4 % Na_2O, 0.4 % K_2O, 7.6 % F) has been estimated to be 0.178 at 1600°C using the FactSage software. This SiO_2 activity allowed calculation of the equilibrium activity ratio of TiO_2 & $TiO_{1.5}$ from the reduction of TiO_2 to $TiO_{1.5}$ by Si in the steel.

$$4(TiO_2) + [Si] = 4\ (TiO_{1.5}) + (SiO_2) \quad (2.18)$$

$$\Delta G^o = -9300 + 2.69\ T\ cal/mol \quad (2.19)$$

And $\frac{a_{TiO_{1.5}}}{a_{TiO_2}} = 1.74$ at 1600°C. The activity of $TiO_{1.5}$ in the slag is almost twice that of TiO_2. The effect of $TiO_{1.5}$ in the slag will be more prevalent than the one of TiO_2. And both titanium oxides will likely affect the behaviour of the molten flux in equilibrium with Ti-stabilised stainless steels.

In a fully aluminium killed steel titania stability, at steelmaking temperatures, can be calculated from the following equilibrium:

$$10\,[Al] + 3\,(Ti_3O_5) = 9\,[Ti] + 5\,(Al_2O_3) \quad (2.20)$$

$$\Delta G^{\circ} = -177385 + 58.39\,T \text{ calories [Sharan et al, 1995]} \quad (2.21)$$

By maintaining [Al] levels in the steel <0.01%, the above reactions can be minimized. This is of importance because it has been found that if attention is not paid to Al levels with regards to maintaining low levels in raw materials and ensuring that no Al is introduced late, supersaturation for the [Al]-[O] solubility product can be reached. This is not desirable for Ti-stabilised steels because Al_2O_3 is not only a major factor in the clogging of the SEN but it is also, with $MgO.Al_2O_3$ spinels, providing the heterogeneous nuclei for TiN, and in the case of the spinel, aid in stabilising the TiN matrix. [Nunnington and Sutcliffe, 2002]

Titania formed by the above reactions will dissolve within the mould slag.
The solubility of TiOx in slags depends on the temperature and the slag chemistry. The following equation has been reported by Nunnington and Sutcliffe [2002]:

$$\%TiO_2 = 77.5608 + 0.00832737 * T(^{\circ}C) - 1.25152 * Al_2O_3 - 0.944873 * CaO - 2.08973 * F - 0.884036 * K_2O - 0.856164 * Na_2O - 0.80930 * SiO_2 \quad (2.22)$$

The regression has the following boundaries: CaO=30 to 40%, Al_2O_3=5 to 15%, SiO_2=30 to 43%, F=5 to 9%, K_2O = 0 to 12 %, Na_2O = 0 to 14% and temperature 1200 to 1475°C. The above equation predicts TiO_2 solubilities of more than 20% at CaO/SiO_2 ratios of <0.8, which is agreement with the work of Kishi and al [1987] and FactSage calculation. Kishi et al [1987], referring to the phase diagram of the system SiO_2-CaO-TiO_2, made the following observations:

- with CaO/SiO_2 ratio = 0.5-0.6 the powder does not enter the $CaTiO_3$ region as TiO_2 content increases to 20 % at 1400°C.
- with CaO/SiO_2 ratio = 1.1 the powder enters the $CaTiO_3$ region as TiO_2 increases, saturation is reached at about 10 % TiO_2 at 1400°C, $CaTiO_3$ (perovskite) is a high melting point phase [Riquier et al, 1997].
- powders in the SiO_2-CaO system with a basicity of 1.4 have a very low solubility for TiO_2 even at 1400°C.

From a FactSage calculation the above observations have been confirmed. It has been found that for a flux basicity of 0.5 there is no perovskite precipitation up to 20 % TiO_2 at 1400°C and for a basicity of 1.2 the flux enters the perovskite region with about 12 % TiO_2.

This means that a large effect of TiO_2 on the viscosity of molten slag can be expected when the basicity of the powder is above 1.1 because of the presence of solid precipitates of $CaO.TiO_2$.

Further FactSage calculations have been done for testing if the presence of fluorine can have an effect on the amount of perovskite precipitating when TiO_2 is added to the flux. A typical composition of a mould flux for an austenitic steel 321 (38 % SiO_2, 36.2 % CaO, 6.3 % Al_2O_3, 8.4 % Na_2O, 0.4 % K_2O, 7.6 % F) and a $CaO-SiO_2$ based flux with 6 % and 10 % TiO_2 has been used for the calculations in the range of temperature from 1400°C to 1200°C. Two basicities have been used, namely 0.95 and 1.2.

As it can be seen on the Figure 2.3 below, the presence of fluorine increases only slightly the mass% of perovskite. For a basicity of 1.2 the mass% of perovskite is about 11 % at 1200°C for 10 % TiO_2 in the flux in presence of fluorine and 10% under the same conditions in the absence of fluorine.

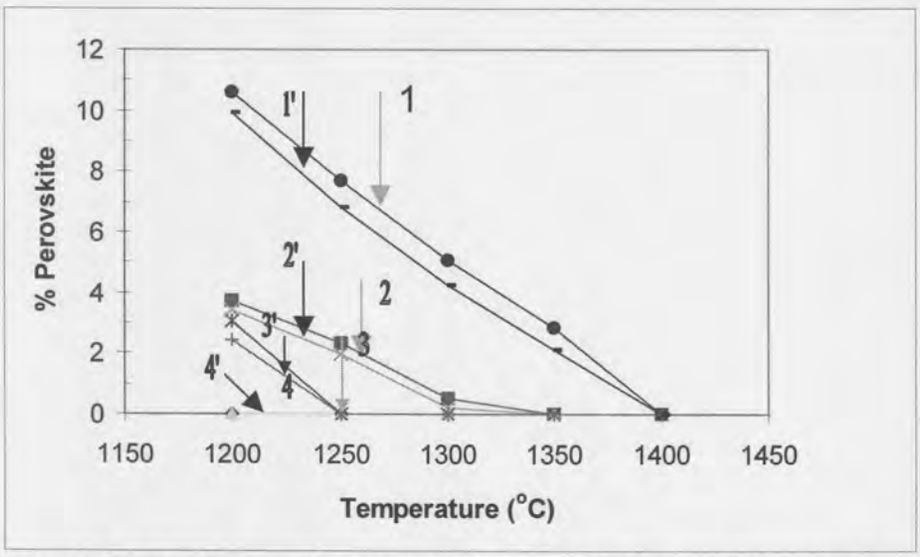

Figure 2.3: *FactSage calculation of the mass % of perovskite in presence and absence of fluorine where 1,2 10% TiO_2; 3,4 6% TiO_2; 1,3 B=1.2; 2,4 B=0.95; ' without F.*

It must also be added that Ti_2O_3 additions to mould fluxes can form another type of perovskite precipitate ($Ca_2Ti_2O_5$) which can form complete and nearly ideal solid solutions with the one formed by TiO_2 ($Ca_2Ti_2O_6$) [Pelton, 2003]. FactSage calculation predicts formation of solid solutions of the two types of perovskites for a mixture of the two titanium oxides. The % of the two perovskite in the solid solutions depends on the TiO_2 and Ti_2O_3 contents in the flux. For example with a total content of 6 % (TiO_2 + Ti_2O_3) in the typical flux for the austenitic steel mentioned above at 1300°C, the % of $Ca_2Ti_2O_5$ in the solid solution increases from 62 % at 10 % Ti_2O_3 content (in the mixture of the two titanium oxides) to 96 % at 90 % of Ti_2O_3 in the mixture. This is also observed with Ti_3O_5 additions in the flux. At a basicity of 1.2, FactSage calculation predicts in this case also formation of solid solutions of the two perovskites. From 1400°C to 1200°C, the mass% of perovskite precipitating increases from 0.21 % to 12.1 % with respectively 86.48 % and 79.28 % of $Ca_2Ti_2O_5$ in the solid solution. It is clear that the mass % of perovskite precipitating increases when the temperature decreases and with additions of Ti_3O_5 or a mixture of TiO_2+ Ti_2O_3 the solid solutions formed are rich in $Ca_2Ti_2O_5$ (> 60%) and the $Ca_2Ti_2O_5$ content decreases with decrease of temperature.
This means with titanium oxides formed during casting the perovskite precipitate is likely a solid solution of $Ca_2Ti_2O_6$ and $Ca_2Ti_2O_5$ perovskites.

2.2. Functions of mould fluxes

The basic functions that a mould flux is required to perform are shown graphically in Figure 2.4; and are as follows [Branion, 1987]:

1. Thermal insulation to prevent partial solidification at the surface.
2. Protection of metal against oxidation by air.
3. Absorption of inclusions rising up to the surface
4. Lubrication of the contact between metal and mould.
5. Promotion of homogeneous thermal transfer adapted to casting conditions.

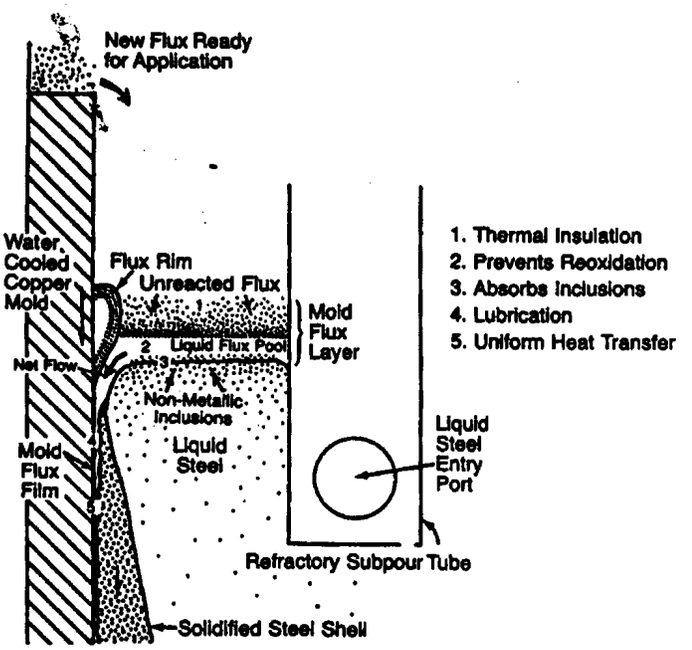

Figure 2.4: *Functions of Continuous Casting Mould Fluxes* [Branion, 1987]

All these functions are essential and an inadequacy in any of them may result in very serious defects. In this part the main conclusions of literature on these basic functions will be discussed. Starting with the first three functions, which are performed by the slag at the surface of liquid metal, the discussion will end with two last functions, which will determine the performance of the slag infiltrated between steel shell and mould.

2.2.1 Functions of the slag at the surface of the liquid steel.

2.2.1.1. Thermal protection of the free surface

The flux provides thermal insulation for the liquid steel in the mould. This will prevent " bridging" or solidification of the upper surface of the steel in the mould [Branion, 1987]. Such solidification of the upper surface of the metal is undesirable. All inclusions rising from the liquid pool would be trapped by the steel crystals, leading to the formation of a crust consisting of metal and oxides. Its entrapment in the strand would lead to very

serious defects. Thermal insulation can be obtained by maintaining a layer of a low-density powder with low surface temperature.
For the flux to provide the optimum insulation it is necessary to maintain a "dark" flux practice [Branion, 1987]. Raw, unmelted flux must cover the entire surface of the mould at all times. Normally a minimum 25mm layer of unmelted flux should be maintained. Additional flux should be added as needed, in small quantities, to keep the surface dark.

Carbon particles help retard the sintering of the powder, and are usually completely burnt before reaching the surface of the metal. Requirements for satisfactory thermal insulation therefore depend only on grain size distribution (whether granulated or loose powder), and carbon content, and not on slag chemical composition. [Riboud & Larrecq, 1979]
In general, low-density fine powders with high carbon content will provide the best thermal insulation. Virtually all fluxes will provide sufficient insulation during normal operations, as such insulation presents few problems. During periods of extended line stoppage for submerged entry nozzle, tundish, and grade changes, it may be advantageous to use highly insulating flux to retard meniscus solidification. [Branion, 1987]

2.2.1.2 Protection against oxidation

The second function of mould fluxes is to prevent re-oxidation of the steel by insulating the steel from the atmosphere.
The flux above the liquid steel meniscus generally consists of three layers –(i) an unmelted, dark unreacted flux layer on top, (ii) a carbon enriched, or perhaps sintered layer, in the center, and (iii) a molten flux layer directly over the steel. The powder is added continuously to the mould to form these three layers. The thickness of these different layers will affect the degree to which the slag can protect the steel from oxidation. Thicker layers will provide more efficient chemical protection.
For correct atmospheric insulation and inclusion absorption the entire meniscus should be covered with a molten flux pool at all times. The depth of liquid pool is also very important in terms of the ability of the flux to flow into the gap between the shell and

mould wall. The minimum depth is oscillator stroke length plus average variation in liquid level to allow for flux to flow over the meniscus during the upstroke. If the liquid flux depth becomes too great, then excessive slag rims can form, which will cause irregular flux flow into the gap. A typical molten flux depth is 10 mm. Also it should be noted that excessive variations of liquid-level in the mould could increase slag rim formation.

Chemical protection is compromised by [Diehl et al, 1995]:
(1) excessive turbulence in the mould when there is a non-uniform flow through the submerged entry nozzle (SEN)
(2) disturbance of the narrow face by a standing wave (which arises because of the steel flow through the SEN); this standing wave tends to expose the molten steel.

Powder design can help to rectify this problem to a certain extent. If the powder consists of spherical particles, the particles can roll down the slope of the standing wave exposing molten slag or steel surface. Expanding granules on the other hand have reduced flowability and will keep the molten metal from being exposed to the atmosphere. Spherical granule with an expending agent is reported to provide the best thermal isolation together with chemical control and minimum flowabitlity [Diehl et al, 1995].

Transport of oxygen from an oxidizing atmosphere through a slag is strongly dependent upon its iron content. It is well understood that the use of powders rich in iron oxide is detrimental to the quality. Most products, at the present time, contain less than 4 % total iron and many of them less than 1%. Therefore, a liquid layer of almost any of these slags is sufficient to fulfill this second function.[Riboud & Larrecq, 1979]

2.2.1.3. Absorption and dissolution of inclusions

The third major function of the slag at the surface of the liquid steel is to absorb harmful inclusions from the steel. The flux assimilates these materials and forms lower melting

point compounds which flow out of the mould with flux. The chemical composition of the flux determines its ability to absorb inclusions.

From a surface thermodynamics point of view, for a solid inclusion arriving at the liquid surface, complete emersion seems to be always possible, whatever the liquid slag composition. Differences between slags appear in the ensuing process of dissolution of solid inclusions in liquid slag [Riboud &Larrecq, 1979].

Failure to dissolve these solid particles as soon as they arrive leads to a heterogeneous slag; the interface may become congested with solids. Among the other detrimental effects, infiltration of slag between steel shell and mould becomes erratic and lubrication deteriorates strongly.

2.2.2 Functions of infiltrated slag between steel shell and mould wall

As said before the performance of a molten flux is determined by its ability to lubricate the contact between steel shell and mould and to allow homogeneous heat transfer adapted to casting conditions. These two functions are greatly affected by slag properties and the most important properties, which govern the behavior of molten flux, are:

- the melting rate
- the viscosity
- the crystallisation temperature

2.2.2.1. Slag properties

1. Melting rate

The melting rate of the flux determines the ability of the flux to maintain stable molten flux depth conditions in the mould. The flux must be added and melted at the rate at which it is consumed. Also, during unstable conditions, such as start-ups, speed changes and tundish changes, the flux must rapidly provide liquid for lubrication.

The melting rate is dependent on flux composition and melting point, flux particle size, shape and the type and amount of carbon added. It decreases with increasing carbon content and decreasing size of the carbon particles. Concerning the type of carbon, Kawamoto [1994] reported that carbon black had a bigger effect than coke.
Free carbon controls the flux melting rate by providing an inert barrier between the solid flux particles and/or liquid droplets and, thus, retarding liquid formation. Carbon sources smaller in size than the flux have a more pronounced effect on melting rate than particles larger than the flux. This is caused by better coating of the flux particles by the finer carbon materials.

Again, the critical factor in terms of melting rate is the ability to maintain a consistent liquid flux depth under the varying conditions normally encountered in casting operations.
In some work conducted at Kawasaki Steel by Sakuraya et al [1987], it has been shown that during speed changes for example, the liquid flux depth drops to one-third the normal value and subsequently returns to normal. During this transient period, flux in-flow is greatly reduced, and, as such, almost no lubrication exists. These conditions can lead to breakouts. By adjusting the flux carbon types and amounts, a more satisfactory performance can be obtained. Also, the melting-rate characteristics must be adjusted so that consistent molten flux depth can be maintained at different constant speeds.

Branion [1987] compared the influence of speed changes on the depth of molten flux for two types of fluxes. As shown in the Figure 2.5 below, the depth of flux type B would decrease to insufficient levels when operating at higher speeds. Flux type A would provide a consistent depth at various speeds.

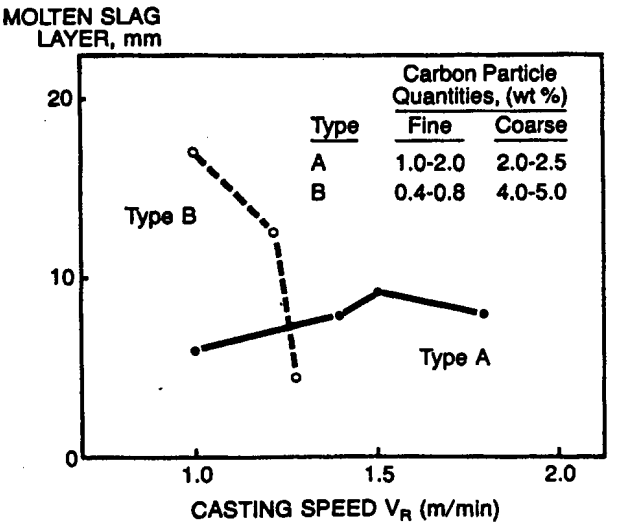

Figure 2.5: *Change of the thickness of molten slag layer with changing casting speed*

When the melting rate is too high, more of the casting powder on top of the mould will melt. This in turn can bring about the formation of a larger rim due to excess of liquid flux during oscillation cycle and partial solidification of the molten steel surface if the powder on the top of steel surface cannot reduce vertical heat flux sufficiently.

The disadvantage of using carbon in mould-flux is carbon pick-up that is experienced during the casting of steels (especially ultra-low carbon steels and stainless steels where low carbon levels are needed).

To compensate this negative effect of carbon, carbonates can be added in the raw materials in addition to carbon especially when higher casting speeds are needed because carbonates increase the melting rate.

Kawamoto et al [1994] found that the melting rate increases as carbonate content increases, which is the opposite of the effect of carbon. A disadvantage of carbonates from the chemical protection viewpoint lies within the decomposition reaction that makes them otherwise favorable - carbon dioxide is a product of this reaction that provides an oxidising atmosphere. Carbonates are then used together with other carbon sources.

2.Viscosity

The viscosity is a measure of resistance of a fluid to flow when subjected to an external force.

As proposed originally by Newton 300 years ago [Mudersbach, 2001], the shear stress, i.e., force per unit area (F/A), causing a relative motion of two adjacent layers in a liquid is proportional to the velocity gradient du/dz, perpendicular to the direction of the applied force,

$$\frac{F}{A}=\eta\frac{du}{dz} \tag{2.23}$$

Where the proportionality factor η is the viscosity of the fluid. Most fluxes and glasses are believed to obey the above equation and are newtonian liquids.

As such, a higher viscosity fluid will require more force at a given velocity gradient.

In honor to Poiseuille, who pioneered the earlier studies of viscosity, the unit of viscosity is called the Poise (P), which is $0.1Ns/m^2$. For lower viscosity, the unit of centipoise (1cP = 0.01P) is often used.

The viscosity of molten flux is primarily determined by its composition and the temperature.

The temperature dependence of viscosity is sometimes represented by Arrhenius equation:

$$\eta = A \exp(E/RT) \text{ or } \ln\eta = \ln A + E/RT \tag{2.24}$$

Where η = viscosity

A= Arrhenius constant

E= activation energy for viscous flow

R= gas constant

T=absolute temperature, ^{o}K

As such, by plotting ln η versus 1/T, a line with a constant slope E/R and intercept, ln A can be expected over a given temperature range.

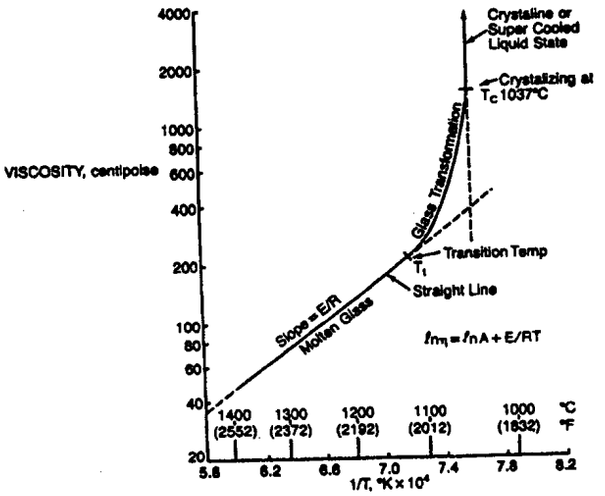

Figure 2.6: *Typical flux viscosity curve [Branion, 1987].*

Figure 2.6 shows a typical curve of flux viscosity (on a logarthmic scale) versus reciprocal temperature, which is composed of the three sections:

- a linear portion with slope E/R at elevated temperature above T_t.
- a curving glass – transformation region from T_t to T_C
- a vertical portion, starting at T_C following crystallization or reaching the supercooled relaxed liquid state of the silica glass.

The Arrhenius representation usually displays a slight curvature for silicates and improved fits can be obtained using the Weymann and Brostow relationships [Mills, 1995]:

- Weymann representation:

$$\eta = A_w T \exp\left(\frac{E_w}{RT}\right) \qquad (2.25)$$

- Brostow representation:

$$\eta = \exp(A_B + \frac{B_B}{T} + C_B \log T) \qquad (2.26)$$

Mould fluxes are usually a polymerized chain network of calcium metasilicate composition for V ratio (wt % CaO/ wt %SiO_2) of 0.65 to 1.20. The basic building block is the $(SiO_4)^{4-}$ silica tetrahedron [Branion, 1987].

The composition of mould fluxes will vary in accordance with the casting conditions, but most have compositions within the pseudo- wollastonite region of the silica-lime-alumina ternary phase diagram. Other oxides such as Na_2O, B_2O_3, MgO, Fe_2O_3 and fluorides such as CaF_2 may be added to control heat transfer and lubrication characteristics.[Johnston & Brooks, 1997]

The ability of an oxide to form a network can be expressed in terms of its local field strength, given by:

$$F = \frac{Z_C}{a^2} \qquad (2.27)$$

F = the field strength

Z_C = the valence of the cation

a = the distance between the centre of the radii of the cation and oxygen ions

A cation with higher field strength (F≈1.5) is more able to attract oxygen anions to achieve a denser packing and become a glass former. Field strengths of ≈ 0.1 – 0.4 characterize network modifiers, which tend to lose oxygen when dissolved in a slag. Network modifiers break up the silicate network of silicate tetrahedra. This causes the network of silica tetrahedra to separate as each tetrhedron can have its own oxygen ion. The cation will be accommodated at the breaks in the silica structure. This results in the formation of discrete molecules which decrease steadily in size as more basic oxides are added to the melts [Johnston & Brooks, 1997].

Fluorine, added either as CaF_2 or NaF, acts as a fluidizer. The addition of fluoride reduces viscosity very effectively. As the radius of F^- (1.31 Å) is similar to that of

O^{2-}(1.38 Å) in tetrahedrally bonded Si-O network structure, F^- can easily replace the divalent oxygen ion resulting in breakdown of Si-O network [Kim et al, 1992]

B_2O_3, a network former, increases the silica chain length which results in an increase in viscosity [Mills, 1995].

In multicomponent slags, Al^{3+} (F = 0.96) assumes a coordination number of 4 and forms tetrahedrons of $[AlO_4]^{5-}$ which are a similar size to the silica tetrahedron $[SiO_4]^{4-}$, so that in such systems alumina is a glass former. In order to substitute Al^{3+} for Si^{4+} in the silica chain and maintain electrical neutrality, the presence of divalent cations such as Ca^{2+} is required. Thus the ability of alumina to increase the silica chain length is dependent upon the concentration of the basic oxides. By this fact, it can be concluded that as the alumina content of a slag increases, so the viscosity increases. And of all the other components that can be added to $CaO-SiO_2$ based slags, alumina is the element that increases the viscosity the strongest [Branion, 1987].

There is a little literature on the effect of TiO_2 on the viscosity of SiO_2-CaO-Al_2O_3 slags. In silica glasses the coordination number of Ti^{4+} (F=1.04) is usually 6 which precludes the formation of a tetrahedron capable of forming a network with silica [Turkdogan, 1983]. Thus TiO_2 will lose oxygen to the silica network and should decrease the viscosity of the slag. In contrast to this, some researchers [Turkdogan, 1983] suggest that the addition of TiO_2 increases the average molecular chain length. However, due to the relative weakness of the Ti – O – Si bond compared to the Al – O – Si bond, TiO_2 should have a relatively small effect on the viscosity.
Johnston & Brooks [1997], measured the effect of TiO_2 addition on the viscosity of two mould fluxes used respectively in continuous casting of ultra low carbon (ULC) steel and medium carbon (MedC) steel. The ULC mould flux had a basicity of 1.1 and TiO_2 content of 0.098 % while the MedC mould flux had a basicity of 1.3 and TiO_2 content of 0.092 %. They found that TiO_2 had a negligible effect on the viscosity of ULC and MedC casting fluxes at low concentrations (< 10 %). At higher concentrations the viscosity of the flux increased sharply [Figures 2.7 and 2.8].

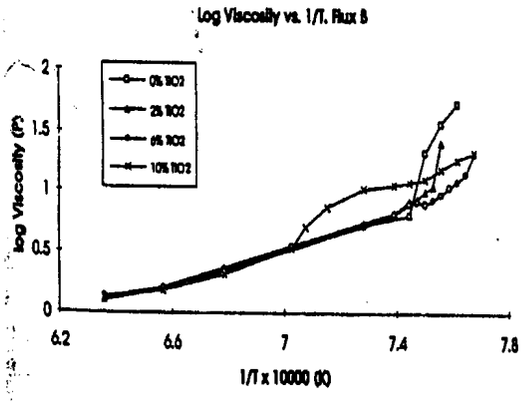

Figure 2.7: *Effect of TiO_2 on the viscosity of the ULC casting flux*

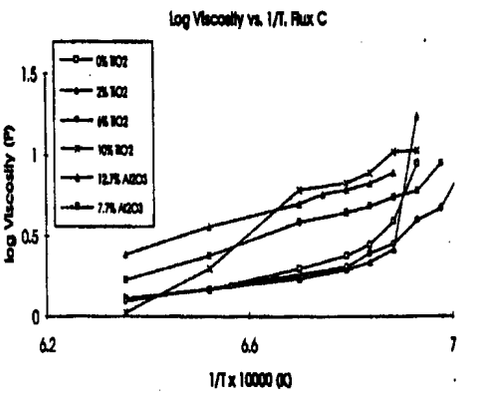

Figure 2.8: *Effect of TiO_2, Al_2O_3 on the viscosity of MedC casting flux*

They attributed this fact to a massive networking and molecular growth and concluded that it should not be necessary to alter casting speed when casting titanium bearing steels unless the TiO_2 content in the flux is approaching 10 % wt.

They apparently did not consider the fact that TiO_2 can form some solid precipitates in the slag and Ti in those steels can form not only TiO_2 but also TiN and other titanium oxides (Ti_3O_5, Ti_2O_3,...). All these titanium compounds can have an effect on viscosity of molten fluxes.

Concerning the formation of solid precipitates by TiO_2, it is confirmed that at higher concentrations, TiO_2 can combine with CaO to form calcium titanate precipitates [Kishi et al, 1987]. Those precipitates are very refractory (melting point 1970°C) and can be responsible for the premature solidification of the steel meniscus and can also perturb the lubrication of the mould with a risk of breakout [Riquier et al, 1997].

This assumption is confirmed in the work conducted by Kishi et al [1987] on the influence of TiO_2 absorption by mould flux used in continuous casting of titanium stabilised stainless steel.

They tested some slags of the SiO_2- CaO or SiO_2-CaO-BaO composition systems and ranged from 0.5 to 1.1 in basicity ($\frac{CaO}{SiO_2}$). They found that when the basicity of the powder is above 1, $CaTiO_3$ precipitates are formed and the flux increases in viscosity (from less than 2 poises to 5 poises) but when the basicity is below 1, $CaTiO_3$ is not

formed and the flux decreases in viscosity (from about 2 poises to 1 poise). During continuous casting of Ti-stabilised stainless steel, when the starting basicity is below 1, it can rise to more than 1 because of the reduction of SiO_2 in the slag by Ti in the molten steel.

It must also be added that TiO_2 is not the only Ti compound, which can form during continuous casting of Ti-stablised stainless steel. We can also have other compounds like TiN, and some titanium suboxides (Ti_3O_5, Ti_2O_3, TiO…) and those compounds can each have an effect on the viscosity of the slag.
As said before TiN can lead to an increase in viscosity due its limited solubility in the slags.
Concerning the effect of the Ti suboxides, Sommerville et al [1982], measured the viscosity of some slags in the $CaO\text{-}SiO_2$ and $CaO\text{-}SiO_2\text{-}Al_2O_3$ systems by using graphite components in the viscometer. This meant that the conditions were reducing, so that part of the effect attributed to TiO_2 may in fact have been due to the presence of significant amounts of Ti_3O_5 or Ti_2O_3.
They found that the production of Ti_3O_5, Ti_2O_3, TiO,… causes an initial decrease in viscosity due both to structural changes and to a lower melting point. With more prolonged reduction, further accumulation of these suboxides past the optimum concentration associated with the minimum melting point, then leads to an increase of viscosity due to decreased superheat.

3. The crystallisation temperature.

In continuous casting of steel, mould powder is added continuously to the top of the mould where it melts to a liquid slag. The slag is then subsequently withdrawn in the gap between the mould wall and the solidifying steel strand, serving as a medium for both lubrication and heat transfer. The slag film closest to the mould, which experiences the highest cooling rate, freezes initially to a glassy layer, whereas the slag film next to the strand remains liquid. Between these two layers crystals will precipitate. The presence of crystals has decisive effects on both lubrication and the heat transfer between the mould

and the strand. It is for this reason that a fundamental understanding of the crystallisation of slags under various thermal conditions is important.

As stated before the viscosity (η) versus the reciprocal of the absolute temperature (1/T) presents a sudden increase in viscosity at a critical temperature during viscosity measurements in cooling down. This phenomena has been named by many authors "break point" (T_{bp}), "crystallisation temperature" (T_C) and "solidification temperature" (T_S).[Kim et al, 1992, Bommaraju, 1991]

From the studies done by Kim et al [1992], there can be two types of break point behaviour (Figure 2.9).

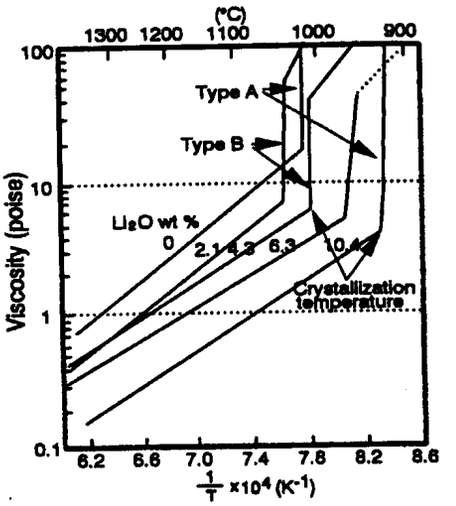

Figure 2.9: *Rheological behaviour of melts around crystallisation temperature [Kim et al, 1992]*

One ("type A") is where the viscosity increases apparently infinitely at the crystallisation temperature, the other ("type B") is where the viscosity increases greatly (3-12 times) at the crystallisation temperature and increases further with a finite slope as the temperature decreases further. To examine these behaviours, Kim et al carried out metallographic and X- ray diffraction analyses on quenched samples of mould fluxes. The existence of these two types of crystallisation behaviour was thought to have a relation with solidification range and crystallisation tendency. The solidification temperature (T_S) for a powder is defined pragmatically as the temperature where the viscosity reaches 100 Poise [Turkdogan, 1983]. It is clear that this temperature has no significance at all to the

crystallisation temperature (T_C or temperature at which the slag starts to form crystals) of the slag since crystals could be precipitating over a temperature interval before this viscosity is reached.

The term solidification temperature has little significance for the flux viscosity behaviour since it is not clearly reflected in the viscosity – temperature graphs. The solidification temperature (T_S) is used to denote that temperature at which the slag becomes solid (that being glass, crystalline or both). T_S cannot be related to T_C in any respect since it contains no information on where the crystals start forming. T_{bp} and T_S on the other hand should be close in casting powders that exhibit a temperature below which the viscosity starts to increase rapidly, since the viscosity will reach 100 Poise near the sharp increase (T_{bp}) of the viscosity. Thus, the term "crystallisation temperature" must not be confused with the solidification temperature of the slag which is determined from viscosity tests [Bezuidenhout, 1999].

It is well known from classical nucleation theory that the onset of the formation of solid crystals in slags must be a function of cooling rate and that to determine the true crystallization behaviour of the slag, isothermal time temperature transformation diagrams (TTT curves) or continuous cooling transformation diagrams (CCT curves) must be constructed. Examples of TTT and CCT curves for a mould slag of composition: wt% CaO 39.58; SiO_2 40.94; Al_2O_3 6.94; Na_2O 9.57 and CaF_2 1%; are given in the Figures 2.10 and 2.11)

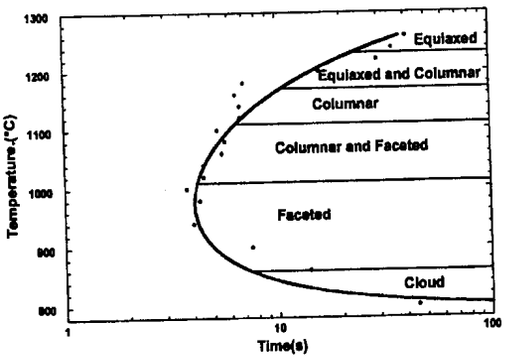

Figure 2.10: *TTT diagram for the onset of of crystallisation [Orrling et al,2000]*

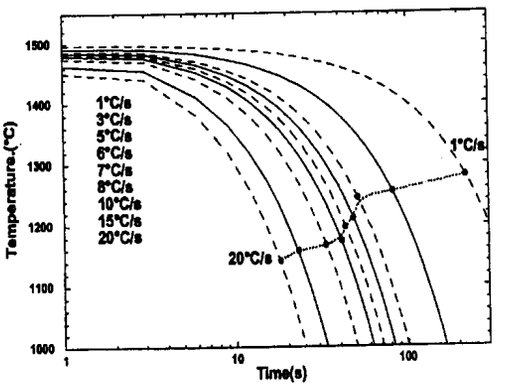

Figure 2.11 *CCT diagram for the onset crystallisation [Orrling et al, 2000]*

Depending on the degree of undercooling different crystal morphologies can be precipitated. The amount of crystalline fraction depends greatly on the cooling rate. Increasing cooling rate drastically reduces the crystalline fraction. In addition, the growth rate, morphology and solidified fraction of the slag under varying cooling rates are important in the determination of the effect of crystallization of the slag on heat transfer and rheology.

Indeed, a strong influence of the gas phase (Ar, air, O_2, wet atmosphere) has experimentally been shown in various oxide systems (aluminate spinel, lithium silicate, etc…) when studying the crystallisation behavior of mould slags in air

[Rocabois et al, 2000]

Concerning the influence of gas phase, Orrling et al [2000] carried out experiments on the effect of the presence of water vapor on crystallisation. By the double hot thermocouple technique, they obtained TTT and CCT diagrams and determined the crystal morphology at different degrees of undercooling or cooling rates. They found that the presence of water vapour increases the nucleation rate and crystal growth rate significantly when compared to experiments carried out in dry atmosphere. This can be seen on the Figure 2.14 for a slag of the same composition as the one quoted above for TTT and CCT curves.

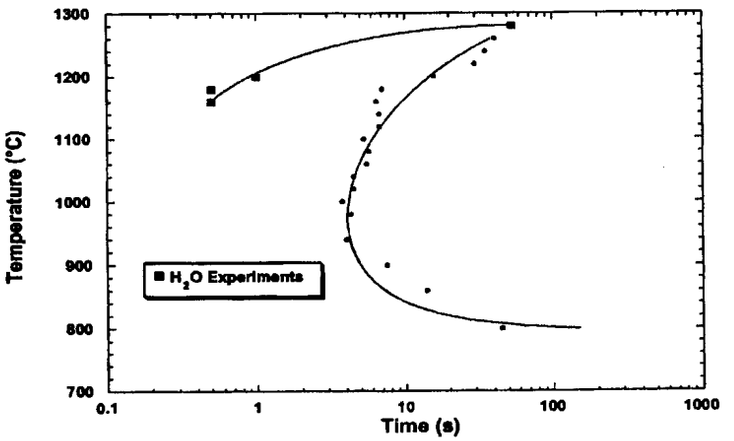

Figure 2.12:*Comparison between isothermal experiments with and without water vapour for a mould flux of composition wt% CaO 39.58; SiO_2 40.94; Al_2O_3 6.94; Na_2O 9.57 and CaF_2 1% [Orrling et al, 2000].*

These results suggest that there is significant interaction between water vapour and liquid slags at high temperatures and the phase diagram for these slags is very sensitive to the equilibrium partial pressure of water vapour in the surrounding atmosphere
[Orrling et al, 2000]
On the effect of mould flux composition on crystallisation temperature, referring to work done by Kim et al [1992], it can be said that the flux composition has a strong effect on crystallisation temperature. The crystallisation temperature decreases with an increase in B_2O_3, F, Li_2O, MgO and to a lesser extent Al_2O_3

For its part, TiO_2 is a well known nucleating agent [Rocabois et al, 2000 & Barbieri et al, 1997], which can be added to batch mixture in order to increase the crystallisation temperature. The nucleation activity of TiO_2 has a double effect. On one hand, Ti^{4+} ($\frac{Z}{a^2_{Ti^{4+}}}$=1.04) which is sixfold coordinated possesses a lower field strength than Si^{4+} ($\frac{Z}{a^2_{Si^{4+}}}$=1.57) which is fourfold coordinated. Ti^{4+} can act as a glass structure modifier to relax the structure, lower viscosity and facilitate other diffusion processes which arise during nucleation or crystal growth. On the other hand, it has been observed that its limited solubility into some glassy compositions and its tendency to create ordered zones with high titania content, as said before in the case of formation of titanates, can be a starting of either a phase-separation process or nucleation. In any case, the presence of a high field-strength cation, such as magnesium, will enhance this behaviour.
Barbieri et al [1996] conducted some experiments in order to test the nucleating effect of TiO_2 during crystallisation of some complex alumino silicate glasses (Li_2O-MgO-ZnO-SiO_2 glass-ceramic system). They confirmed the great effect of TiO_2 on glass nucleation. This was possible by a simple optical observation of all the treated glasses. This effect was visible as a change in color, and crystallisation, visible as opalescence. They observed also that as a trend, a shift of 50 °C toward higher temperatures from the undoped to 2 mol% addition and from the latter to 5 mol%. Also, the crystallisation tendency increased with an increase in Li_2O content.

For their part, Rocabois et al [2000] studied the effect of TiO_2 or ZrO_2 addition to crystallisation kinetics. They tested the addition of TiO_2 or ZrO_2 as nucleating agents in complex mould compositions containing less than 30% of SiO_2. They found that it does not decrease the time of appearance of first crystals and the overall crystallisation rate is only slightly increased.

It can be concluded that the effect of TiO_2 as a nucleating agent is not always observed.

2.2.2 2.Relations between slag properties and performances.

1. Influence of slag properties upon lubrication.

The fourth major function of molten flux is to provide lubrication between the solidifying shell and the mould wall.
Molten fluxes infiltrate into the annular space between the mould and the steel shell. The performance of this infiltrated flux is determined by its viscosity and crystallisation temperature.
The frictional force which the steel strand experiences as it is drawn through the mould is a measure of the lubrication which the strand enjoys.
In work conducted by Riboud et al [1979], friction force measurements were carried out on slab casters. The global forces applied on the mould, resulting from the slab extraction, were in the range of 5000 Newton per square meter of contact. Computed friction forces, for hydrodynamic lubrication conditions, are in the range of 20 to 500 Newton per square meter of contact for various slags known to be used in continuous casting. This strongly suggests that in some parts of the mould, solid-solid friction takes place. This is in agreement with observations of copper wear in the lower part of the mould. The fact that the global forces applied on the mould, resulting from the extraction, do not show detectable variations with slab size, argued for the presence of preferential solid-solid friction zones. At different locations in the mould, hydrodynamic slag lubrication or solid-solid friction could be prevalent.

In the upper part of the mould, high temperatures and fairly uniform pressure, transmitted by the steel shell at a given level, offer good conditions for hydrodynamic lubrication with liquid slag films. In this region where the metal shell is the thinnest and has particularly low strength, friction forces would depend almost exclusively upon the value of slag viscosity at the temperature of the contact with steel (1500 – 1400°C in this region). Low viscosity slags are recommended for high speed casting. Interruption of the film could be caused by unsatisfactory feeding conditions at meniscus level; severe danger of breakout would then arise.

Near to the exit of the mould, more particularly on narrow faces of slabs, the steel surface temperature may become so low that the slag behaves like a solid, even in contact with the steel shell. Shear takes place at the solid-copper interface and erosion occurs on the copper plates. To prevent this low melting point slags would be desirable.

The increase of friction resistance between the mould and the shell can provoke the sticking of the mould and the solidifying of shell which is responsible for break-out (B.O.). B.O. is one of the major problems in the continuous casting operation, and it is well known that the frequency of the sticking type B.O. increases at high casting speeds [Kyoden et al, 1987]. The viscosity and crystallisation temperature of the mould powder have an important effect on the occurrence of the occurrence of the sticking type B.O. Kyoden et al [1987] investigated the relationship between physical properties of mould slags (viscosity and crystallisation temperature) and the frequency of the sticking type B.O. in actual operation. They tried four mould powders at casting speed between 1.2 – 1.6 m/min. As shown in Table 2.6, the mould powders with a high crystallisation temperature showed a high frequency of sticking type B.O. This result suggests that the crystallisation has some influence on the lubricating function of the powder slag or heat transfer. On the other hand, the viscosity of the mould powder showed no influence in this investigation, which the authors attributed to the small range of viscosities of the four powders.

Table 2.6: *Breakout frequency by Powders [Kyoden et al, 1987]*

	A	B	C	D
Crystallisation Temperature(°C)	1010	1020	1060	1080
Viscosity at 1300° C (Poise)	1.5	3.2	2.4	1.6
B.O frequency (%)	0.0	0.0	0.64	2.32

In work conducted by Orrling et al [2000], industrial observations suggested that increased moisture content of mould powders can cause increase friction between mould wall and in some cases dramatic increase in B.O. The increase of friction is presumably due to the precipitation of solid crystals in the molten slags.

According to Imai et al [1986], many types of gas bubbles such as argon and hydrogen are considered to pass through the powder pool until they are diffused toward the surface close to the meniscus. They found that the crystallisation of the mould powder is increased with an increasing amount of gas bubbles present in the slag [Figure 2.13]. The index of crystallisation in higher basicity ($CaO/SiO_2 = 1$) greatly increased. The index of crystallization remained constant in lower basicity ($CaO/SiO_2 = 0.9$) powder. The viscosity also sharply rises with increasing gas bubbles in the slag, which deteriorates the lubrication properties between the mould and the shell [Figure 2.14]. The use of appropriate mould powder that is not so greatly affected by gas bubbles will maintain lubrication effectively to prevent breakout caused by sticking.

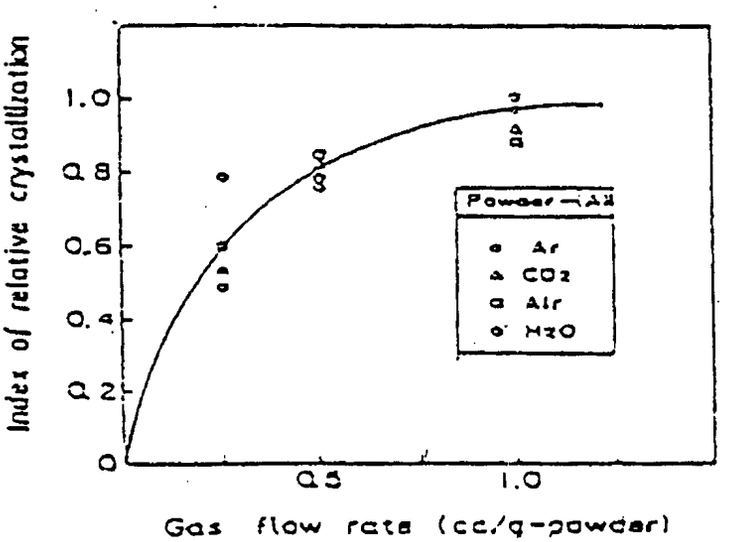

Figure 2.13: *Influence of gas flow rate on powder crystallisation [Imai et al, 1986].*

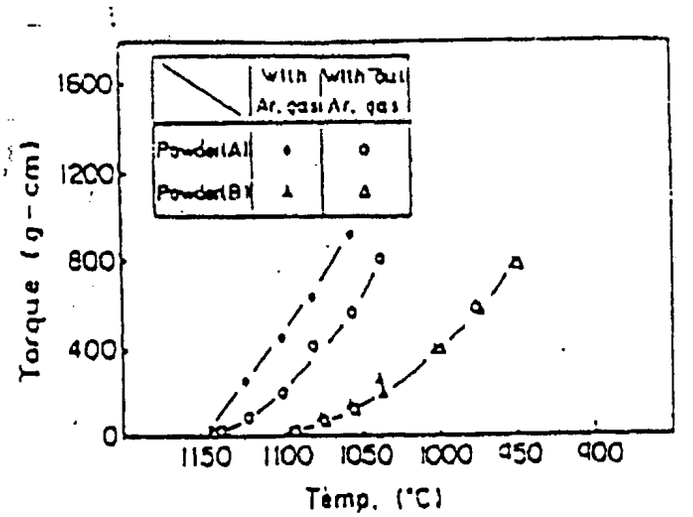

Figure 2.14: *Influence of Argon gas on lubrication of mould powder [Imai et al, 1986].*

2. Influence of slag properties upon heat transfer.

The last major function of molten flux is to provide uniform heat transfer between the solidifying shell and mould wall. Heat transfer across the interfacial gap greatly affects steel quality. The uniformity of this initial heat transfer rate, as well as its magnitude is very important [Thomas et al, 1999]. Non uniform heat transfer generates thermal

stresses in the shell, which are worsened by differences by differences in thermal contraction of γ austenite and δ ferrite. This produces non-uniform shell growth, which leads to a variety of quality problems including deep oscillation marks (and subsequent transverse cracks), localized hot, weak regions which concentrate strain and form longitudinal cracks, and surface shape problems such as rhomboidity of billets [Brimacombe et al, 1998]

In the extreme, breakouts may occur when the mould wall does not match the shell shrinkage. Insufficient taper (related to unexpectedly high heat transfer) might cause an air gap, where regions of the shell become too weak to support the liquid pool below the mould. Excessive taper (related to unexpectedly low heat transfer) might cause jamming of the shell in the mould [Thomas et al, 1999]. These problems are best avoided by understanding and controlling heat transfer across the interfacial gap.

The rate of heat transfer across the interfacial gap depends mainly on the properties including lattice (or phonon) conductivity (k_c) and radiation conductivity (k_r) [Mills et al, 2002], and contact resistances, especially where the flux is solid.

In terms of heat transfer, the following general items can be stated
[Branion, 1987]:

1. the heat transfer is controlled in three steps:
   (a) steel shell to flux
   (b) through flux
   (c) flux to mould wall
2. a liquid flux against the shell provides maximum heat transfer in this area.
3. A 100 percent solid flux provides the lowest heat transfer due to air gaps being present at both 1a and 1c locations.
4. Since a thinner total flux film thickness t exists with more fluid fluxes, then a higher heat transfer would be expected with these.

From a large number of heat flux measurements carried out on several continuous casting moulds, it can be deduced that the main casting parameters controlling the heat extraction are the casting speed and the nature of the lubricant [Brimacombe et al, 1979]

In Figure 2.15, we can clearly see that the maximum heat flux increases with decreasing viscosity.

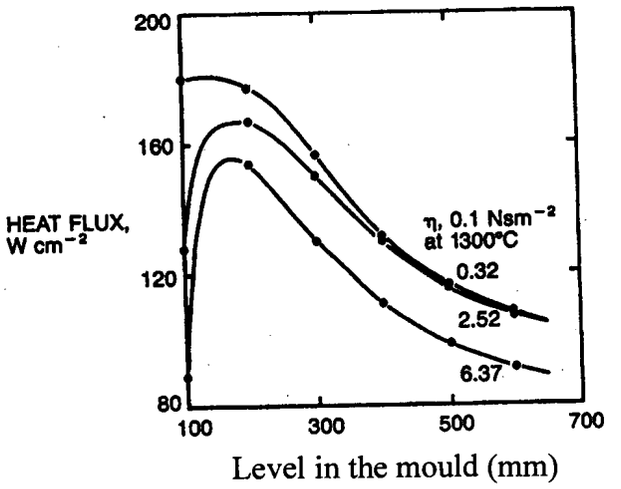

Figure 2.15: *Heat flux as a function of viscosity* [Branion, 1987]

Figure 2.16 presents some results obtained on slab casting mould [Riboud & Larrecq, 1979]. Heat flux density is plotted as a function of casting speed for three different powders ($\eta_1 > \eta_2 > \eta_3$)

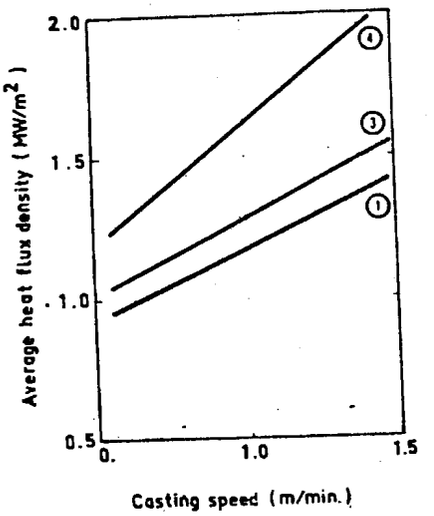

Figure 2.16: *Average heat density measured for several casting speed Numbers 1,2 and 3 refer to different mould fluxes* [Riboud, 1979].

The heat flux density increases with the casting speed and the influence of casting powder can easily be seen on this figure. This is observed practically: the change of powder type during a cast can be detected directly on the mould cooling water temperature recordings [Riboud, 1979].

Riboud et al [1979] carried out other experiments for studying thermal balances at various level in the mould, using heat fluxes, at various levels in a mould, measured with thermocouples.

The usual heat transfer calculations consider one single thermal contact resistance between steel and copper. This resistance may be decomposed into three parts (Figure 2.17)

- a thermal contact resistance between solid steel and slag, r_2;
- the thermal resistance arising from the slag layer (of thickness "h" and thermal conductivity "λ");
- a thermal contact resistance between slag and copper, r_1

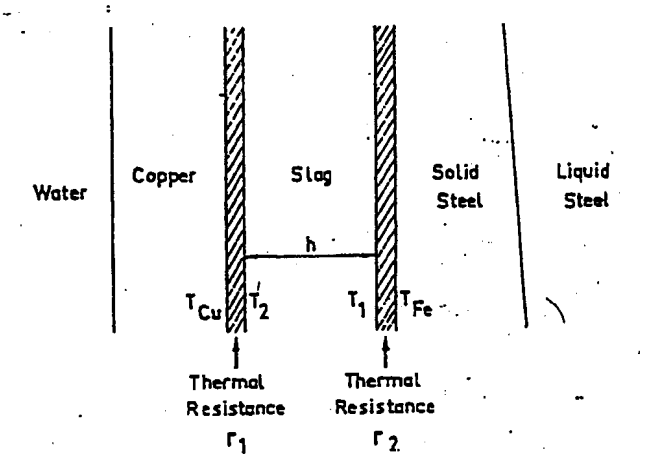

Figure 2.17: *Thermal contact resistance between steel shell and copper mould [Riboud & Larrecq, 1979].*

From measurements of local heat flux density, "Φ", and of steel shell thickness "h", one can compute the surface temperatures of both copper "T_{Cu}" and steel shell "T_{Fe}". One can deduce the relation characterizing heat transfer in the slag;

$$\Phi = \frac{T_{Fe} - T_{Cu}}{r_1 + \frac{h}{\lambda} + r_2} = \frac{T_1 - T_2}{\frac{h}{\lambda}} \qquad (2.28)$$

T_1 and T_2 are the temperatures on the two faces of the infiltrated slag film. The contact resistance "r_2", between solid steel and liquid slag is relatively small; the slag surface is assumed to be at the same temperature as the solid steel shell at its contact ($T_1 = T_{Fe}$).

The contact resistance between slag and copper, "r_1", is always very high compared to r_2. Its value decreases from about 10^{-3} to 5.10^{-4} °C.W^{-1}.m^2, when the slag surface temperature in contact with copper, T_2, increases from 800° to 1200 °C [Riboud & Larrecq, 1979]. A temperature difference of 500 to 700 °C exists between slag and copper ($T_2 - T_{Cu}$), its value depending upon the slag film thickness.

The slag layer is acting as a thermal resistance between shell and mould. Slag behaviour is governed by its viscosity and thickness. "Fluid" slags (low viscosity, low crystallisation temperature), can only form very thin film (< 0.1 mm total thickness). The thermal resistance of this slag is always low. Susa et al [1994] obtained thermal conductivities in the order of 2 W/m.K at 600 °C and about 2.5 W/m.K at 1000 °C for different types of slag samples taken from a mould.

Slag thickness and heat flux density can also be controlled by the powder melting, when using more viscous slag.

Slags that start to crystallise at a relatively high temperature (>1100°C) upon cooling give thicker films in the lower part of the mould (Figure 2.18). Trials were made on a continuous caster with several slags having similar viscosity – temperature curves in their liquid state: a decrease in heat transfer to the mould was observed upon changing the type of slag, going from a low to high crystallisation temperature. This is because of a larger interfacial thermal resistance for slags with high crystallisation temperature (> 1100°C).

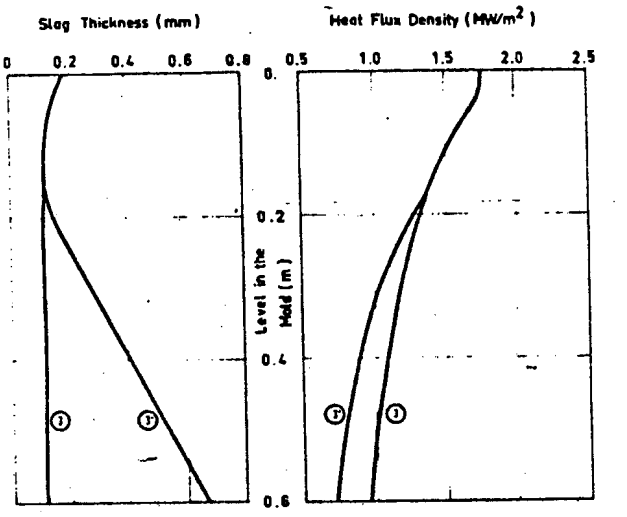

Figure 2.18: *Influence of the crystallisation temperature upon the maximum Slag thickness profile and heat flux densitySlag 3 has a crystallisation temperature below 1100° C and slag 3' is an hypothetic slag having the same viscosity as 3 but 1200° C as crystallisation temperature* [Riboud & Larrecq, 1979]

3. EXPERIMENTAL

Two separate areas of the behaviour of casting powders were experimentally investigated:

- the level of Ti pick-up by the mould fluxes and chemical and phases analyses of the molten flux sampled from industrial casting machines.
- the effect of Ti pick-up on the viscosity of the mould fluxes

This has been done for two mould fluxes:

- LCP1 used for the casting of a ferritic steel type 409
- RF1 used for the casting of an austenitic steel type 321

The chemical composition of the 2 casting powders are given in the Table 3.1 below:

Table 3.1: Chemical composition (in wt %) of mould fluxes used

Powder Name	**SiO_2**	**CaO**	**Al_2O_3**	**MgO**	**Na_2O**	**K_2O**	**TiO_2**	**Fe_2O_3**	**F**	**C**
LCP-1G	37.0	30.2	6.07	1.1	10.9	0.507	0.186	1.89	6.06	2.92
Syntherm RF 1	38.0	36.2	6.3	0.7	8.4	0.4	-	1.2	7.6	4.5

It is evident that the basicity of the flux for the austenitic steel is markedly higher than for the ferritic steel. Although the basicity – expressed as the ratio $(CaO)/(\%SiO_2)$ – is smaller than 1 for both fluxes before use, loss of SiO_2 (through reaction with dissolved titanium or titanium nitride) is expected to increase the basicity during use, enhancing the possibility of perovskite formation upon titanium oxide pick-up.
This effect will be evaluated later.

3.1 . Measurement of Ti pick-up during continuous casting

Samples of molten fluxes were collected by plant personnel from the mould of a continuous casting machine at Columbus Stainless (Middelburg, South Africa). The

sampling in this case was done by means of a small sampling scoop used to collect molten slag by pushing away the powder layer.
All the samples were taken midway between the narrow side left and the submerged-entry nozzle (SEN).

The mould flux consumption for the plant is almost the same for the ferritic and the austenitic steels, about 0.20-0.30 kg/m^2. The oscillation characteristics of the casting machines are respectively as follows: negative strip factor = 1.4 and 1.27, oscillation frequency = 188 and 193 cycles/min, stroke length = 4 mm for both, casting speed = 1.05 to 1.1 m/min.

The chemical analysis of the samples collected was done using Energy Dispersive X-Ray Analysis (EDX), called also Energy Dispersive Spectrometry (EDS), and X-Ray Fluorescence (XRF). The phases analysis was done using the Scanning Electron Microscopy (SEM) and X-Ray Diffraction (XRD).

3.2.Viscosity measurements

The effect of TiO_2, Ti_2O_3 and Ti_3O_5 absorption on the viscosity of mould fluxes of the ferritic and the austenitic steels has been assessed. The amount of Ti oxide additions was 2, 6 and 10 % by weight. Pure TiO_2 and Ti_2O_3 (>99 %) from Aldrich Chemical (U.S.) were used while Ti_3O_5 were obtained by mixing the stoichiometric amounts of TiO_2 and Ti_2O_3.
The viscosity was measured from 1400°C to 1200°C using rotational viscometry technique.
This range of temperature has been chosen to guarantee a homogeneous liquid before the crystallisation of the molten flux starts. When the crystallisation starts the molten flux becomes a heterogeneous mixture of liquid and crystals. This leads to a sudden increase in viscosity with falling temperature and viscosity data of this range are no longer reliable.

Figure 3.1 shows a photo the experimental set-up:

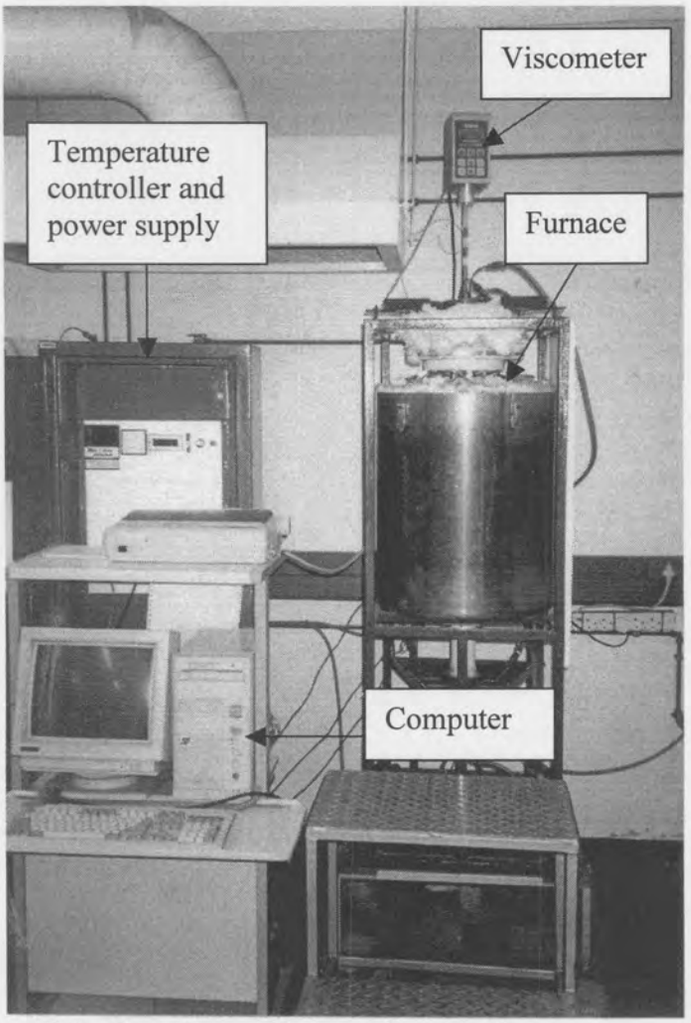

Figure 3.1: *Experimental set-up showing the viscometer on top of the furnace*

3.2.1. Sample preparation

Samples used for the viscosity measurements were prepared by mixing different amounts of pure Ti oxides powder with a commercial casting powder.

Prior to mixing, the casting powder was decarburised at 600°C for 10 hours in air in a muffle furnace. This was done because carbon contained in the flux can hinder viscosity measurements. After decarburisation the powder changed in colour from black to white. About 50 g of the mixed powder was then compacted into a 304 stainless crucible (outside diameter 32 mm, inside diameter 28 mm and 60 mm high).

After viscosity measurements, the crucible was destroyed by means of a hydraulic press and the slag removed. Half of the solid slag was mounted in epoxy resin and polished for SEM/EDX analyses. The other half was milled in a tungsten carbide mill to yield powder samples for XRD and XRF analyses.

3.2.2. Apparatus employed

3.2.2.1. Viscometer

A Brookfield Programmable LVDVII+ Viscometer with electronic display was used in this project for all viscosity measurements. The concentric cylinder method was employed. In this method the viscosity is determined from measurements of the torque generated when one of the cylinders is rotated at a constant speed.

The viscosity (η) is calculated by equation [Mills, 1995]:

$$\eta = \frac{M}{8\pi^2 n h}\left(\frac{1}{r_i^2} - \frac{1}{r_o^2}\right) \qquad (3.1)$$

Where M is the torque, n the number of revolutions per second, h and r_1 the height and radius of the inner cylinder and r_o the radius of the outer cylinder.

The above equation applies to infinitely long cylinders and it is normal practice to calibrate viscometers of these types with viscosity reference materials at both room and high temperatures [Mills, 1995].

Viscosities are usually calculated by the following equation:

$$\eta = \frac{D}{G} = D * \left(\frac{1}{G}\right) \qquad (3.2)$$

Where D = scale deflection of the viscometer

G = apparatus constant determined by calibration experiments.

The viscometer was calibrated at room temperature with Brookfield standard oils of known viscosity of 96.5 cP and 995 cP at 25°C and with pure glycerol.

The calibration consists in the determination of the apparatus constant G at different rotation speeds.

For calibration purpose the viscosity of Brookfield fluids and glycerol were confirmed by using a 600 ml beaker, Brookfield spindles and guardleg. During viscosity measurements with Brookfield viscometer, for maximum accuracy the display reading of the viscometer should be between 10 and 100 %.

The fluids were subsequently tested separately in a stainless crucible, which was the same as the one used for high temperature viscosity measurements. For all the fluids used the torque has been measured at different speeds and the apparatus constant has been determined for each rotation speed (see values of G in Appendix 1).

In order to establish the accuracy of the viscosity data obtained at high temperatures in the furnace, the viscosity of a synthetic reference slag supplied by the National Physical Laboratory (NPL), UK was measured and the results were compared to those of other laboratories. The results are shown in the Figure 3.2.

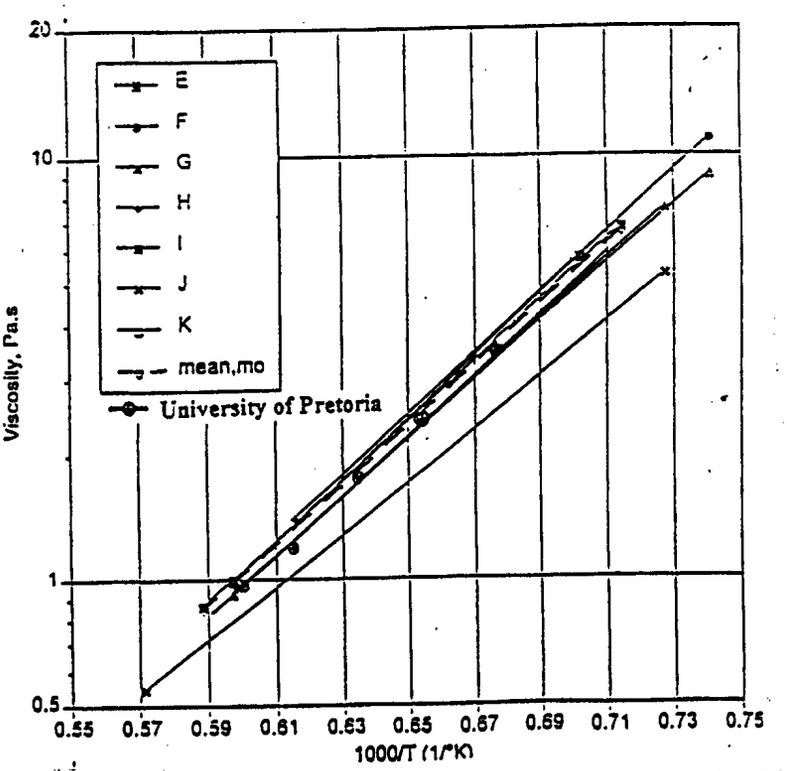

Figure 3.2: *Viscosity of a synthetic reference material supplied by NPL Laboratory, UK. [Mills, 1994].*

3.2.2.2. Furnace

A high-temperature furnace was used for the measurements. The furnace had specially designed silicon carbide elements that can heat the furnace to 1500°C and the furnace was controlled by a controller using a S-type thermocouple situated between the elements. The crucible containing the mould powder was placed in an alumina reaction tube (outside diameter 70 mm and inside diameter 59 mm) mounted vertically inside the furnace. The ends of the alumina tube were sealed with water-cooled copper heads. The spindle extension passed through a small hole in the top copper head. The crucible was supported on an alumina tube (with outside diameter 26 mm) passing through the bottom copper head. Fitting into this tube was placed a mullite crucible holder. Fitting into this again was another mullite crucible for the purpose of acting as a reservoir crucible for slag that sometimes crept out of the stainless crucible due to surface tension effects. On occasion the slag creeping out of the crucible damaged the crucible support, passing through and damaging the sample thermocouple. The amount of slag creeping out of the crucible was markedly reduced by fitting a machined stainless-steel baffle to the top of the crucible (see Figure 3.3).

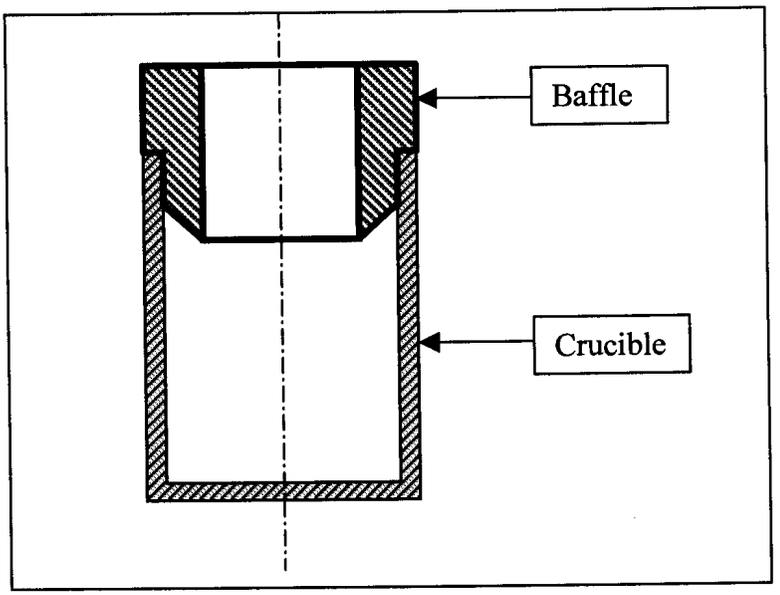

Figure 3.3: *Stainless steel baffle on top the crucible preventing the creeping of the slag from the crucible.*

An S-type thermocouple in an alumina sheath was placed in contact with the bottom of the crucible so that the slag temperature could be measured accurately during the experiment.

The schematic configuration of the inside of the furnace is given in the Figure 3.4 below:

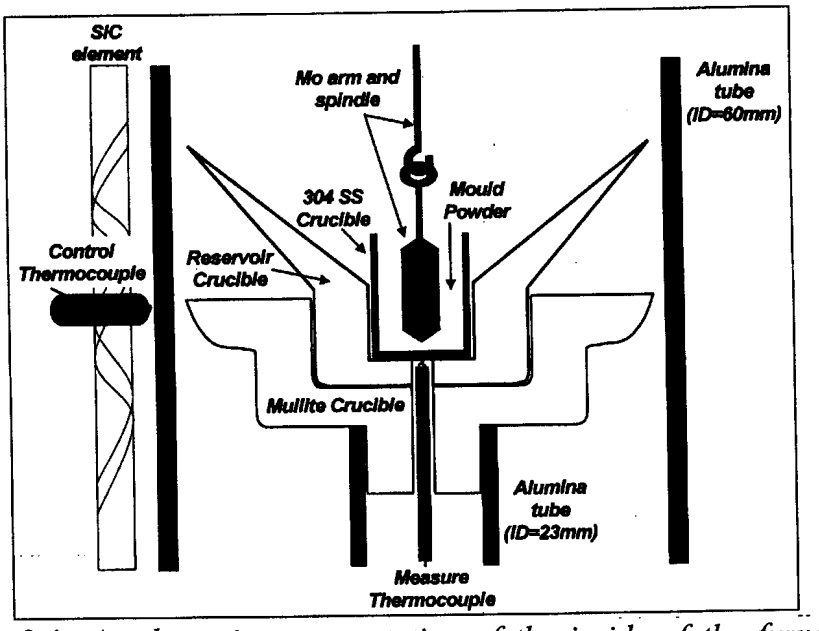

Figure 3.4: *A schematic representation of the inside of the furnace to illustrate the mounting of the sample and position of the spindle and thermocouple [Bezuidenhout, 1999].*

The viscometer was rigidly mounted on the top of the furnace and had to be always adjusted to be aligned to the crucible.

Since the spindle and its extension from the viscometer were made of molybdenum, and the sample crucible made from 304 stainless steel, the oxygen partial pressure in the furnace had to be kept at low levels. This was achieved by flowing argon through the furnace. The argon entered the furnace at the bottom copper head (at rates of 2 litres per minute) and into a small chamber above the top copper head (at rates of 0.02 litres per minute), flushing the opening for the spindle in the top copper head. Before entering into the furnace the argon gas was purified in respect to oxygen and water content to aid in keeping the oxygen partial pressure low. The argon gas passed first through a Drierite

tube (outside diameter 35mm, length 350mm filled with Drierite) at room temperature to strip the gas of moisture. The gas was further passed through a silica tube (outside diameter 40 mm, length 1000mm) containing copper turnings at 600°C to remove the traces of oxygen. At 600°C any oxygen in the argon gas passing through the tube will react with copper to form CuO. The CuO was occasionally regenerated to copper by passing CO through the silica tube at 600°C.

The path of the gas flow is given in the Figure 3.5:

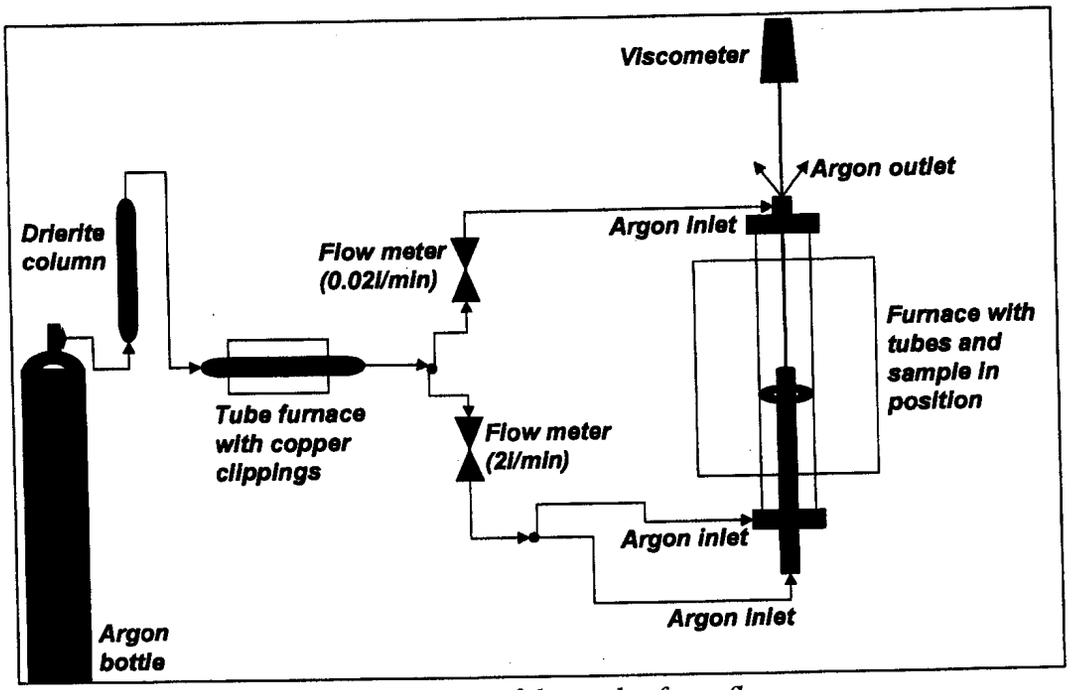

Figure 3.5: *Schematic representation of the path of gas flow*

3.2.3. Experimental procedure

A crucible containing the casting powder was first placed in the central part of the furnace. Before any run, the alignment of the spindle and the crucible had to be checked carefully because if the alignment is not well done the spindle will not be well centred in the crucible and will not rotate properly.

After being sure of a good alignment, the furnace was then closed and the temperature brought up to 1400°C at a rate of 120°C per hour. At this temperature, 2 hours was

allowed for thermal equilibrium to be established. When the temperature was stabilised, the spindle was lowered into the molten flux and the first viscosity measurement was taken at 3 or 4 different rotation speeds. The values of viscosity calculated for these different rotation speeds were generally identical (newtonian behaviour).

After this the furnace was cooled down at 50°C per half an hour and held at each new temperature for 20 minutes to reach steady state (using 50°C intervals). The viscosity was then measured and remeasured for 3 or 4 different rotation speeds. The measurements were stopped when the temperature of 1200°C was reached. The furnace was heated again to 1350°C in order to lift the spindle out from the sample and after that the furnace was programmed to cool down at 120°C per hour to room temperature.

The furnace was then opened, and the spindle and its extension removed.

The slag sticking to the spindle after viscosity measurements was removed with a dilute solution of HF.

4. RESULTS AND DISCUSSION

4.1. Molten flux analysis

The two different aspects of the behaviour of the casting powder are presented:

- Electron backscattered images of the flux sampled from the continuous casting mould.
- The change in TiO_2 and SiO_2 content with casting time in the sampled flux.

4.1.1. SEM/EDX analysis of solidified molten fluxes sampled during casting

Figures 4.1 shows the SEM back-scattered electron images of the glassy and crystalline regions for the mould flux of the ferritic steel and Figures 4.2 shows the same for the mould flux of the austenitic steel.

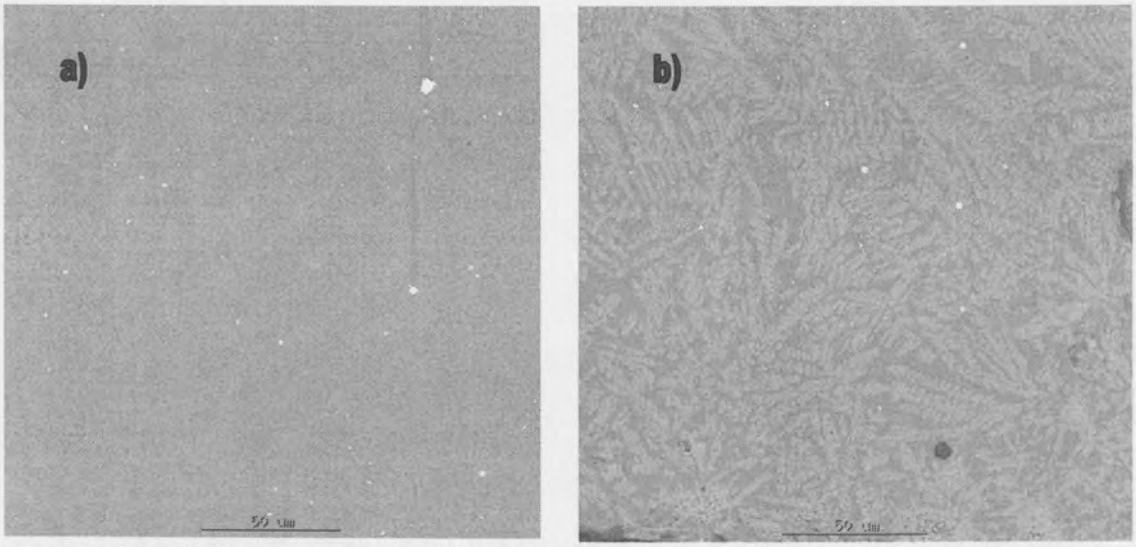

Figure 4.1: *a) Glassy region and b) crystalline region of the mould flux for ferritic steel*

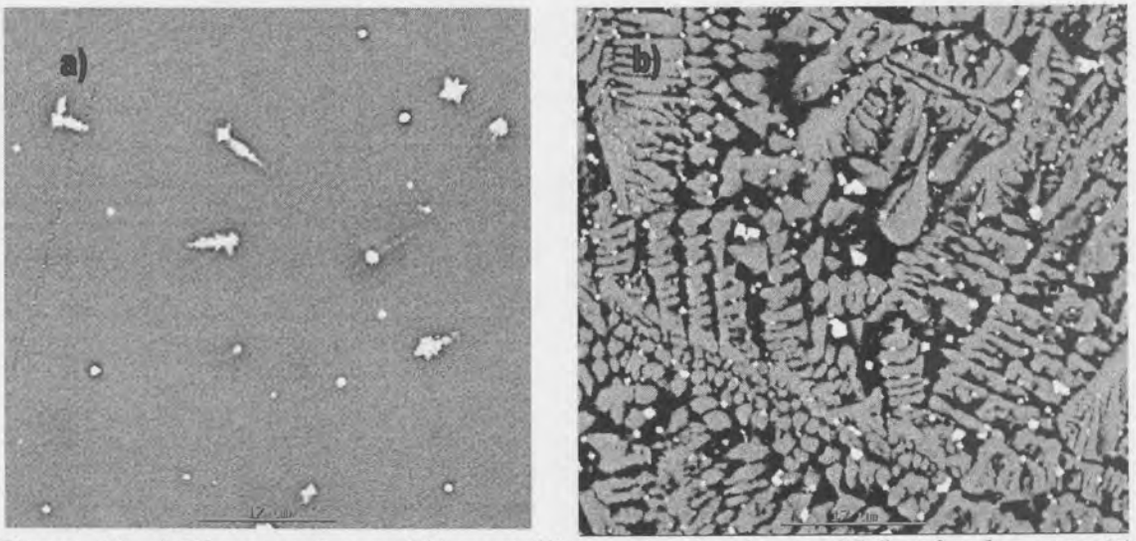

Figure 4.2 *a) Glassy region and b) crystalline region for the mould flux for the austenitic steel*

For both fluxes there is only slightly differences in the average compositions between the glassy and the crystalline areas. These two regions appearing after solidification of the flux indicate that the individual areas have solidified in different ways (glassy and crystalline/dendrite), which would seem to indicate local temperature differences in the liquid phase and hence differences in solidification rates.

It can be seen on this images that for the mould flux of ferritic steel only some spherical metallic droplets can be noticed in the glassy region while in the crystalline two main phases are present.
The two phases are respectively cuspidine (light) and anorthite (dark).
There is no visible formation of Ti compounds.

For the mould flux of the austenitic steel apart from the spherical metallic droplets, a separate solid phase can be seen in the glassy region (see Figure 4.2.a). The EDS analysis of that solid phase reveals that this phase rich in Ca, Ti, and O, and hence this could be the perovskite ($Ca_2Ti_2O_6$ or $Ca_2Ti_2O_5$). The XRD analysis did not give any evident peak indicating the presence of perovskite, but this may be as a result of the small volume fraction of this phase.

In the crystalline region two main phases are present (see Figure 4.4). Cuspidine is the light phase and nepheline is the dark phase. In the crystalline region the presence of some precipitates rich in Ca, Cr, Ti and O was also noticed. This difference in composition for Ca-Ti-O based phase in the glassy and crystalline regions implies that during the cooling the metallic particles are interacting with some oxides in the slag to form Ca, Cr, Ti, O based precipitates.

The spherical metallic particles were found to contain Fe (45 to 75 %) and Cr (35 to 60%) and did not contain Ni. The high Cr content and the absence of Ni means that those particles are not trapped in the slag directly from the molten steel. One suggestion is that these droplets might originate from the oxidation of Cr from the metal phase and its reduction as well as the reduction of FeO at the interface between the slag and the carbon-rich sintered layer. This confirmed the observations made by Scheller [2002] in his work on the redox reactions in slags during continuous casting of stainless steel. He stated that some elements (Cr, Mn) are oxidised from the liquid steel and due to convection flows in the slag layer, the reaction products are distributed in the slag layer and transported to the sintered casting powder layer, where they are reduced by C to form metal droplets.
During cooling those small metal particles act as crystallisation nuclei for slag solidification or accumulate in interdendritic regions. This occurs in the gap between the solidifying strand shell and the mould wall. They thus affect physical properties of the slag during the casting process and also, via the crystallisation effect, the heat transfer.

4.1.2. Change in TiO_2 content with casting time

Figures 4.5 and 4.6 show the evolution of TiO_2 and SiO_2 contents of the ferritic steel mould flux with casting time and Figures 4.7 and 4.8 show the same for the austenitic mould flux.

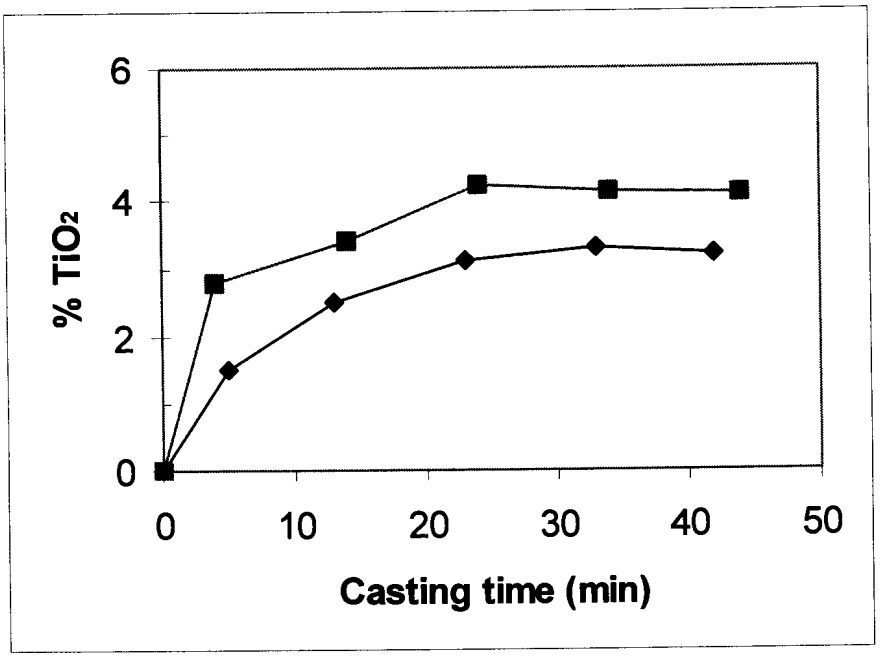

Figure 4.5: *Change in TiO_2 content of the ferritic steel mould flux during casting. Different symbols refer to different casts.*

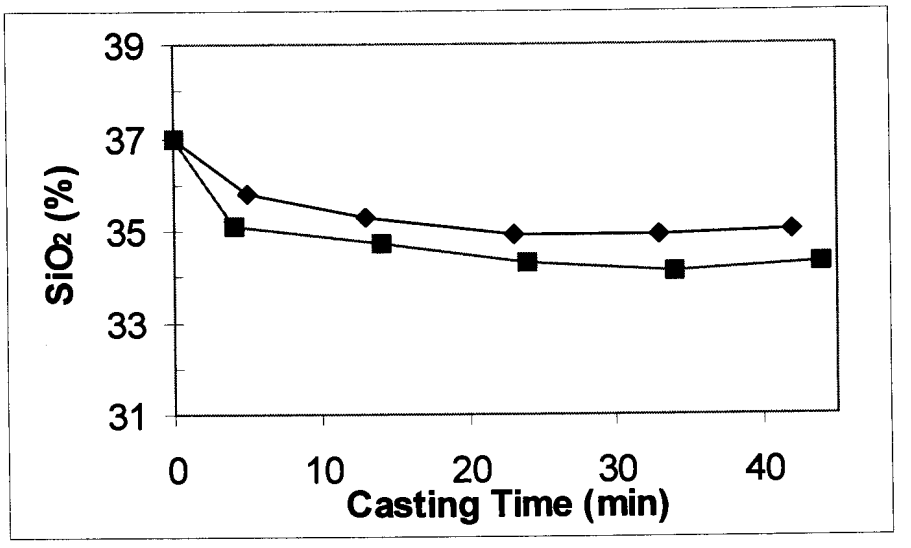

Figure 4.6: *Change in SiO_2 content of the ferritic steel mould flux during casting. Different symbols refer to different casts.*

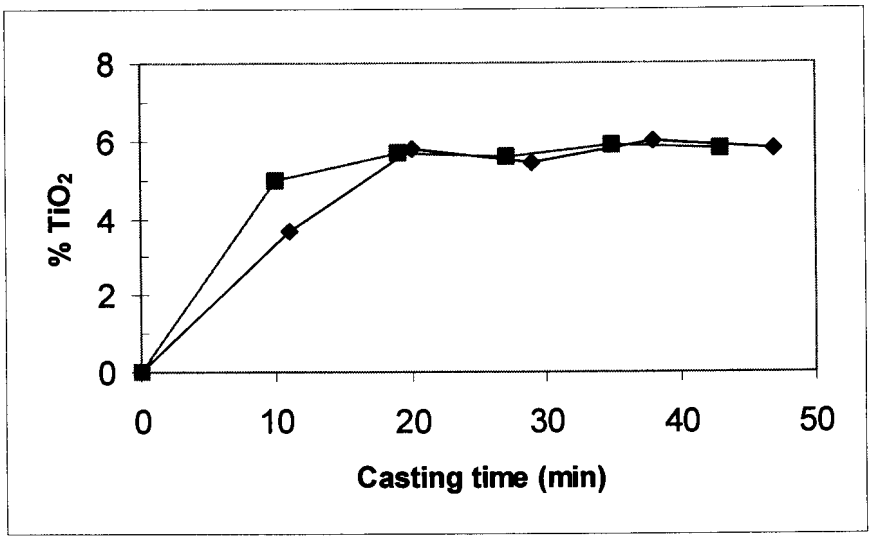

Figure 4.7: *Change in TiO_2 content of the austenitic steel mould flux during casting. Different symbols refer to different casts.*

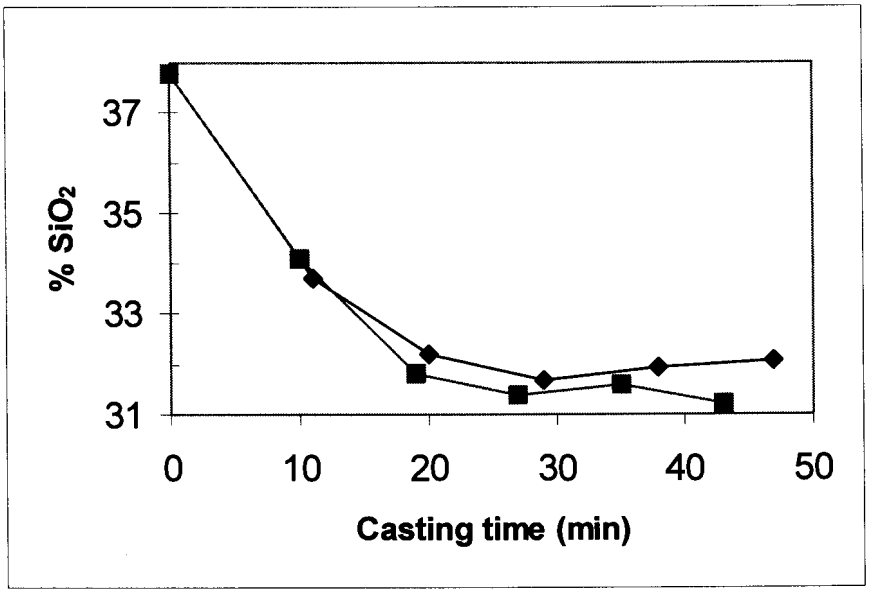

Figure 4.8: *Change in SiO_2 content of the austenitic steel mould flux during casting. Different symbols refer to different casts.*

While the concentrations of the other components of the mould flux stayed roughly constant, both the titanium oxide content (here expressed as TiO_2) and the silica content changed significantly (see Appendix 2). The increase in titanium content and decrease in silica are more marked for the austenitic stainless steel (figures 3 and 4). In both cases, steady-state compositions are achieved within 20 minutes of the start of the cast. This behaviour is similar to that observed previously for aluminium pick-up by carbon steels (Bezuidenhout, 2000). In that work, it was shown that the time constant of the change in composition is approximately equal to the time required for one exchange of the pool of molten mould flux (through flux consumption and replacement by fresh powder).

The larger titanium pick-up for the austenitic steel is in line with the greater propensity to titanium nitride precipitation in that steel, as discussed in the section 2.1.1.

Given the low solubility of titanium nitride, the absence of titanium nitride as a separate phase implies that the titanium is present in the mould flux as an oxide; titanium pick-up by the mould flux hence occurred by one of the following reactions:

$$TiN_{(s)} + (SiO_2) \rightarrow (TiO_2) + [Si] + 0.5\,(N_2)_g \quad (4.1a)$$

$$TiN_{(s)} + 0.75\,(SiO_2) \rightarrow (TiO_{1.5}) + 0.75\,[Si] + 0.5\,(N_2) \quad (4.1b)$$

$$[Ti] + (SiO_2) \rightarrow (TiO_2) + [Si] \quad (4.2a)$$

$$[Ti] + 0.75\,(SiO_2) \rightarrow (TiO_{1.5}) + 0.75\,[Si] \quad (4.2b)$$

The two reactions (4.1a) and (4.1b) reflect oxidation of solid titanium nitride by silica (which is present in the mould flux), to yield titanium oxide (respectively TiO_2 and Ti_2O_3) which dissolves in the mould flux. The two reactions (4.2a) and (4.2b) are for the direct oxidation of dissolved titanium by silica. Clearly, whatever the reaction route, a constant ratio of TiO_2 pick-up to SiO_2 loss is expected. On a molar basis, this ratio is 1:1 if titanium is present in the mould flux as TiO_2, and 1:0.75 if titanium enters the flux as Ti_2O_3.

To test whether a constant ratio is indeed observed, the data of Figures 4.5 and 4.6 are replotted in Figure 4.9 and 4.10, to show the relationship between TiO_2 pick-up and SiO_2

loss. Also shown on the Figures 4.9 and 4.10 are the predicted relationships, if titanium is present in the mould flux as respectively TiO_2 and Ti_2O_3.

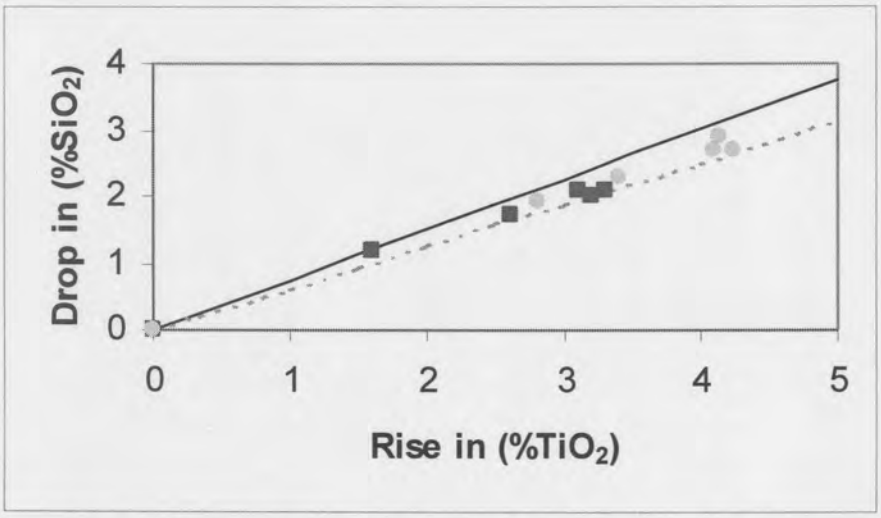

Figure 4.9: *Relationship between drop in SiO_2 and rise in TiO_2 contents for the ferritic steel mould flux. Different symbols refer to different casts. The solid line isthe predicted relationship if titanium enters the flux as TiO_2, and the broken line if the titanium is present as Ti_2O_3.*

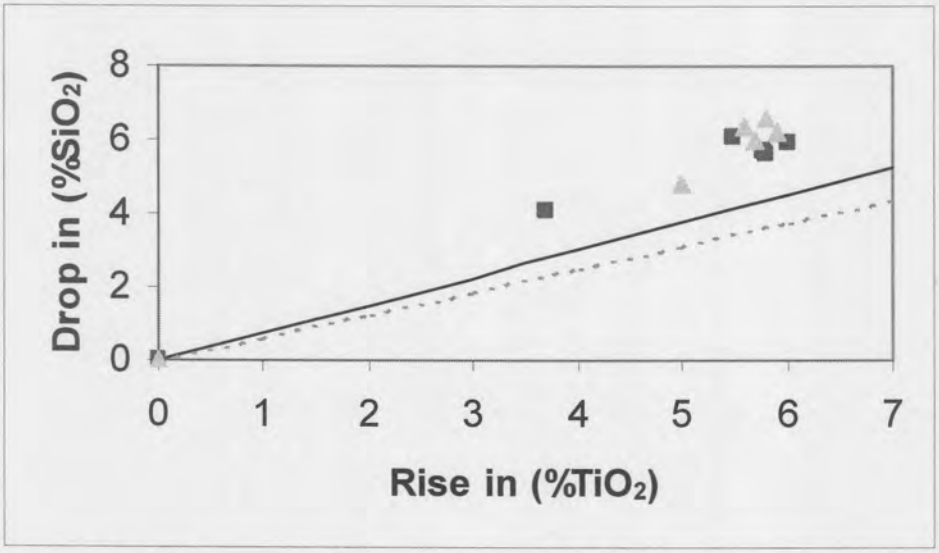

Figure 4.10: *Relationship between drop in SiO_2* and *rise in TiO_2 contents for the austenitic steel mould flux. Different symbols refer to different casts. The solid line is the predicted relationship if titanium enters the flux as TiO_2, and the broken line if the titanium is present as Ti_2O_3.*

Evidently, the data for the ferritic steel follow the predicted relationship well (for titanium as a mixture of TiO_2 and Ti_2O_3). In contrast, for the austenitc steel the loss in silica is larger than predicted by the reactions (4.1) and (4.2). This implies that the mould flux in these cases has one or more parallel mechanisms for loss of silica from the mould flux. Possibilities include the reduction of silica by chromium in the steel, and by manganese. Evaporation of silicon nitride is not considered to be a likely loss route, since the larger loss of silicon occurs with the flux of the austenitic steel, which operates at a lower temperature and has a higher basicity (and evaporation is favoured by higher temperatures).

These results emphasise that greater difficulty with loss of lubrication is likely with the austenitic steel, for several reasons. First, a larger amount of TiO_2 pick-up is found (some 6% compared with 3-4% for the ferritic steel); second, the basicity of the mould flux of this steel is higher, which implies a greater danger of perovskite precipitation and hence increase in apparent viscosity; third, the basicity of the mould flux is increased (from 0.95 to 1.2) by the greater loss of silica during titanium pick-up.

The measured effects of such compositional changes on the mould flux viscosity are presented in the next section.

4.2. Viscosity measurements

The effect of TiO_2, Ti_2O_3 and Ti_3O_5 absorption on the viscosity of the mould fluxes of the austenitic and the ferritic steels was assessed. The amount of Ti oxide addition was 2, 6 and 10 wt% and the viscosity was measured from 1400°C to 1200°C.

Figures 4.11, 4.12 and 4.13 show the effect of TiO_2, Ti_2O_3 and Ti_3O_5 on the viscosity of the mould flux for the ferritic steel while figures 4.14, 4.15 and 4.16 show the same on the viscosity of the mould flux for the austenitic steel.

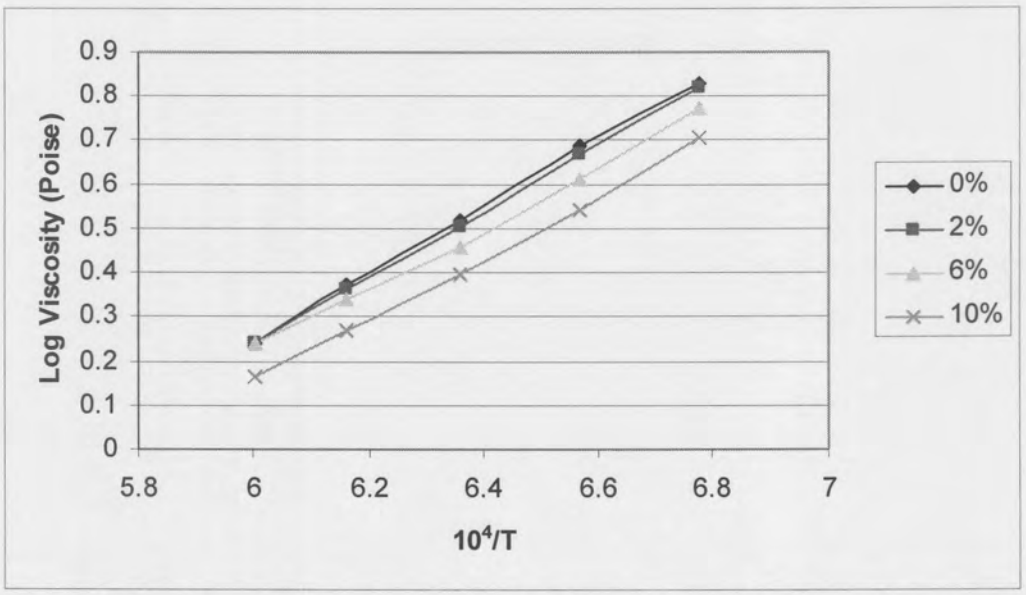

Figure 4.11: *Viscosity change of the ferritic steel mould flux with temperature and increasing TiO_2 content*

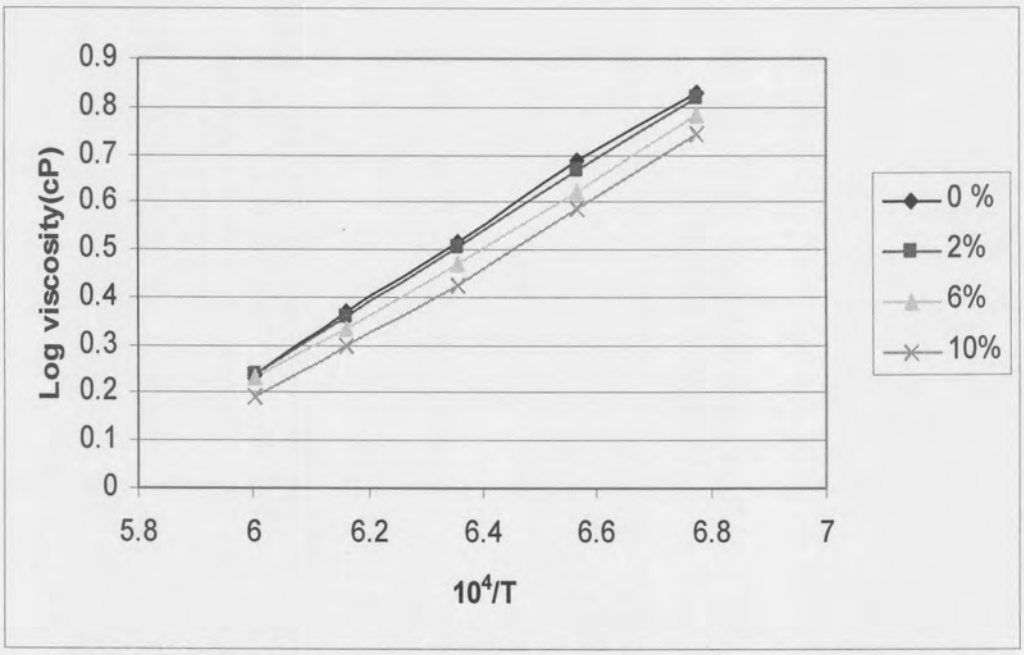

Figure 4.12: *Viscosity change of the ferritic steel mould flux with the temperature and increasing Ti_2O_3 content*

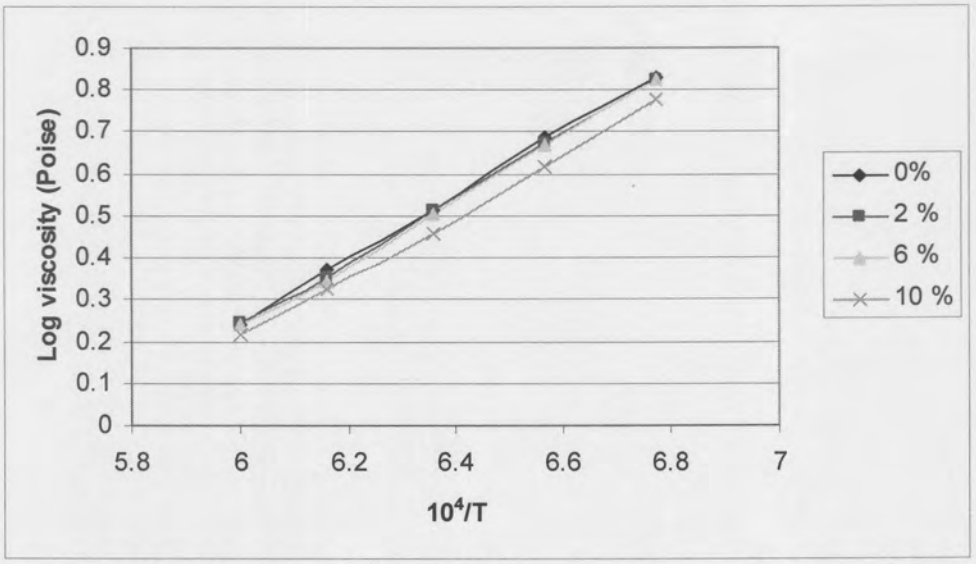

Figure 4.13: Viscosity *change of ferritic steel mould flux with temperature and increasing Ti_3O_5 content*

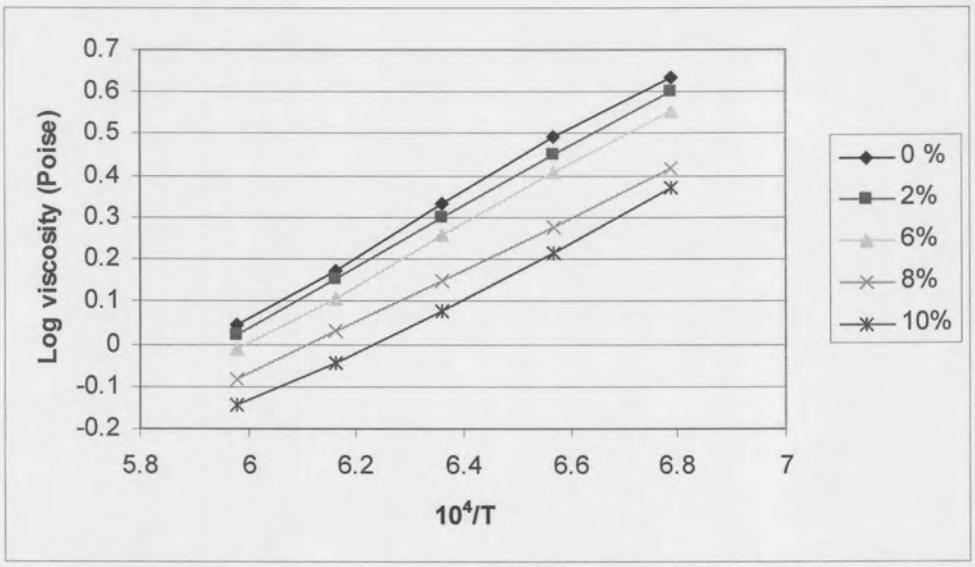

Figure 4.14: *Viscosity change of the austenitic steel mould flux with temperature and increasing TiO_2 content*

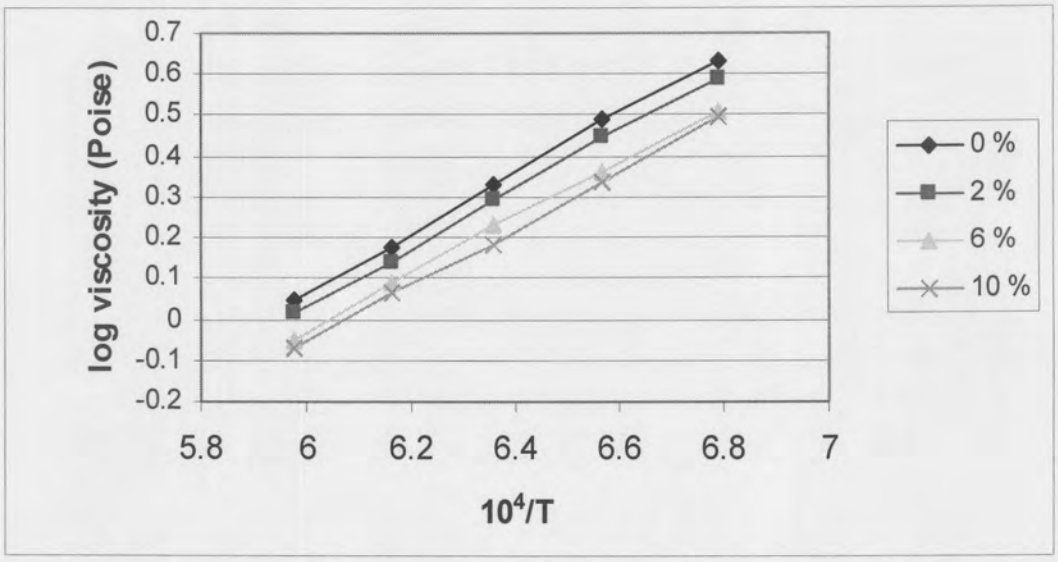

Figure 4.15: *Viscosity change of the austenitic steel mould flux with temperature and increasing Ti_2O_3 content*

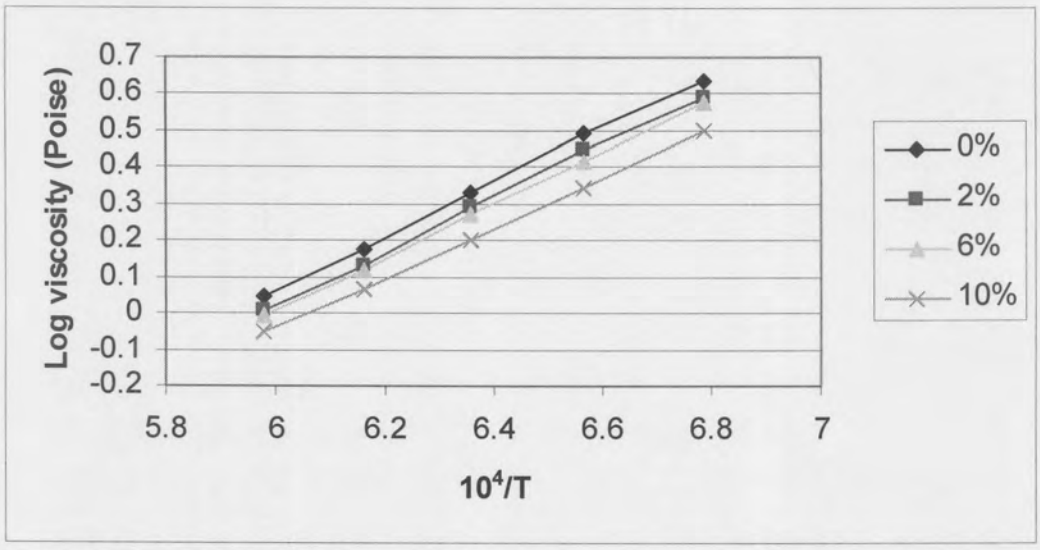

Figure 4.16: *Viscosity change of the austenitic steel mould flux with temperature and increasing Ti_3O_5 content*

As it can be seen in these figures, in both cases TiO_2 decreases the viscosity of the flux across the range of temperature tested. This behaviour of Ti can be understood as said before by the weakness of Si-O-Ti and Ti-O-Ti bonds compared to Si-O-Al and Si-O-Si. Titanium oxides act here as slag thinners.

The slightly lower viscosity of the mould flux for austenitic steel is consistent with the higher basicity of this flux – see Table 3.1.

The same trend has been observed with Ti_2O_3 and Ti_3O_5 additions but the effect of TiO_2 in decreasing the viscosity seems to be slightly stronger than those of Ti_2O_3 and Ti_3O_5. For example, with 10 % of titanium oxide, at 1200 ^{o} C, the viscosity of mould flux for the ferritic steel decreases from 675cP to 507cP for TiO_2 while it is decreasing from 675 cP to 551cP in the case of Ti_2O_3.

To compare the effect of titanium oxides on the viscosity for the two fluxes, activation energies for viscosity flow have been calculated as shown in the Figures below:

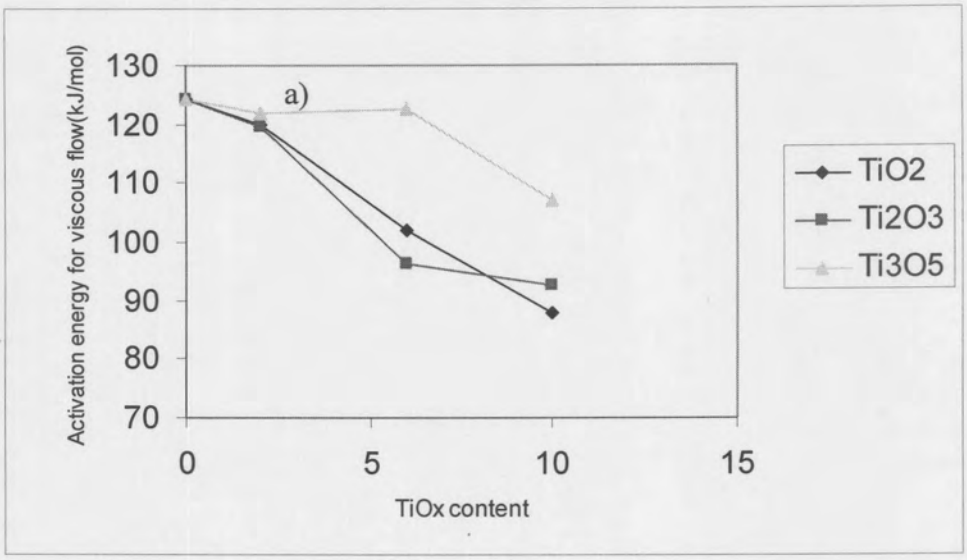

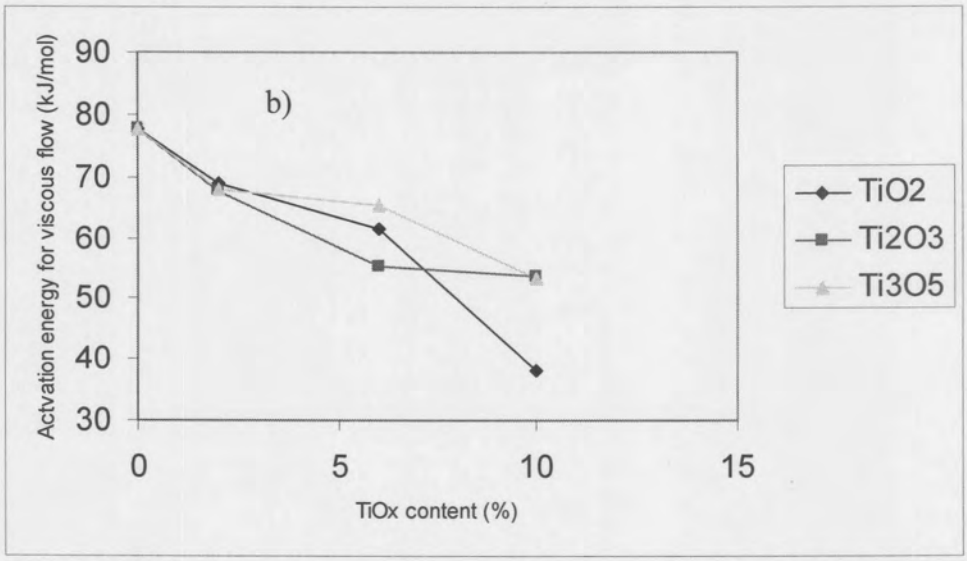

Figures 4.17: *Effect of TiOx content on the activation energy for a) mould flux for ferritic steel and b) mould flux for austenitic steel*

All these three titanium oxides lower the activation energy very effectively. This means in both cases titanium oxides act as network modifier. The effect of Ti_2O_3 seems to be slightly stronger than TiO_2 up to 6 % but in both cases TiO_2 has the strongest effect on the activation energy at 10%. The activation energy decreases from about 80 kJ to 40 kJ when TiOx content increase from 0 to 10 % for the mould flux of the austenitic steel while it decreases from about about 125 kJ to 90 kJ in the same range of TiOx content for the mould flux of the ferritic steel.

All the titanium oxides tested are acting as slag thinners. And at lower basicities (<1), increases in titanium oxides content up to 10 % are not at all detrimental to mould flux viscosity for temperatures from 1400°C down to 1200°C.

The SEM image of the solidified fluxes after viscosity measurements are shown in the figures below:

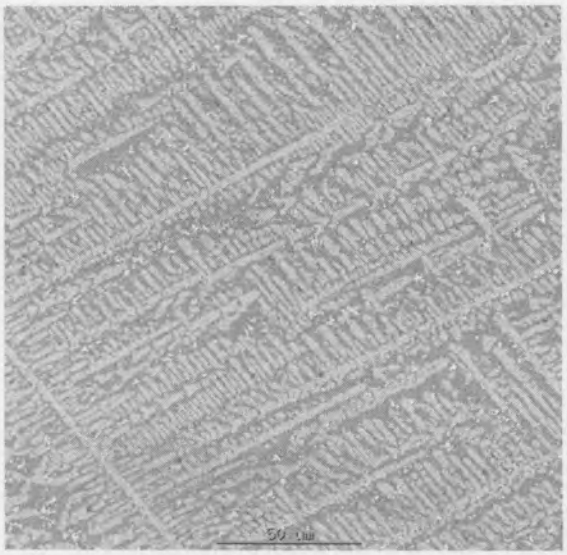

Figure 4.17: *SEM backscatterd image of The mould flux of the ferritic steel without addition*

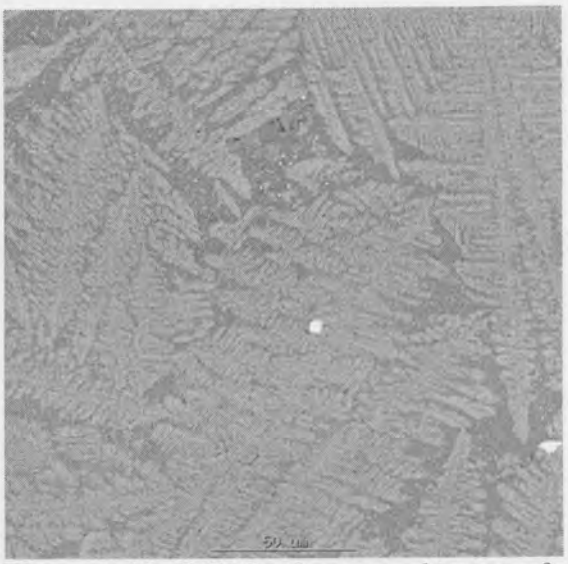

Figure 4.18: *SEM backscattered image of the mould flux of the ferritic steel with 10 % TiO_2*

Figure 4.19: *SEM backscattered image of the mould flux of the ferritic steel with 10% Ti_2O_3*

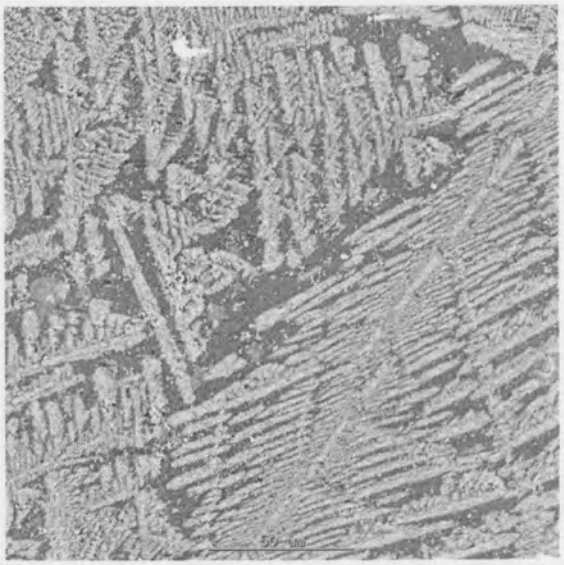

Figure 4.20: *SEM backscattered image of the mould flux of the ferritic steel with 10 % Ti_3O_5*

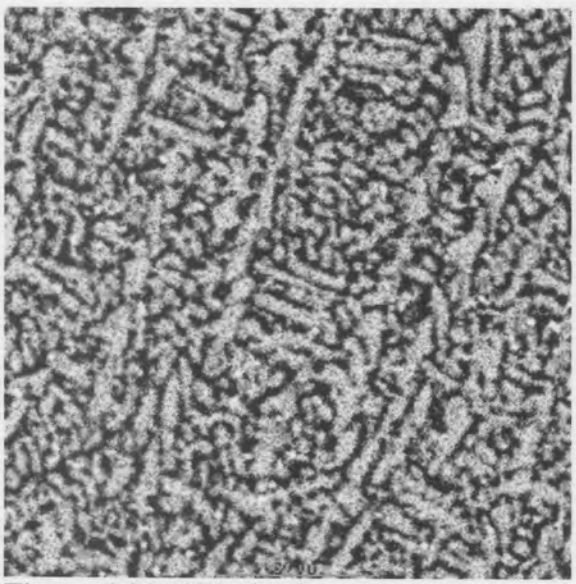

Figure 4.21: *SEM backscattered image of the mould flux of the austenitic steel without addition*

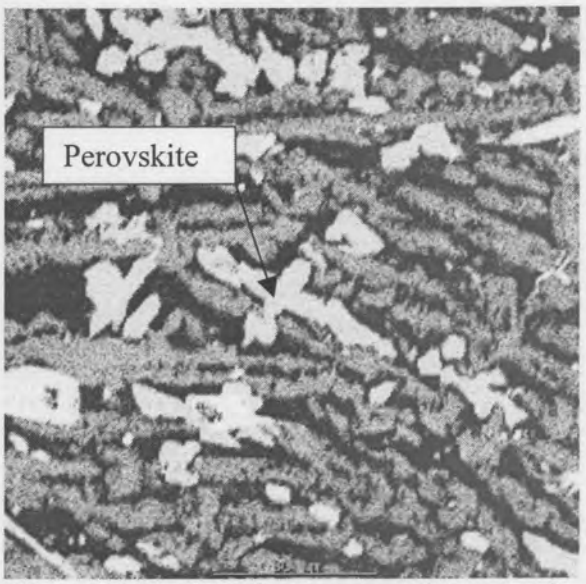

Figure 4.22: *SEM backscattered image of the mould flux of the austenitic steel with 10% TiO_2*

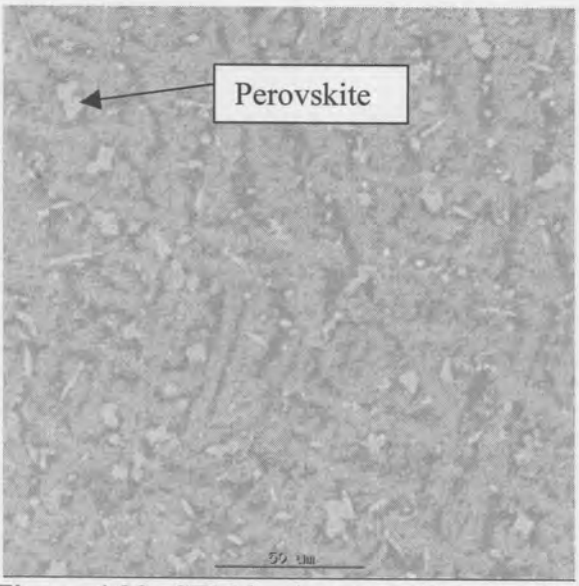

Figure 4.23: *SEM backscattered image of mould flux the of the austenitic steel with 10 % Ti_2O_3*

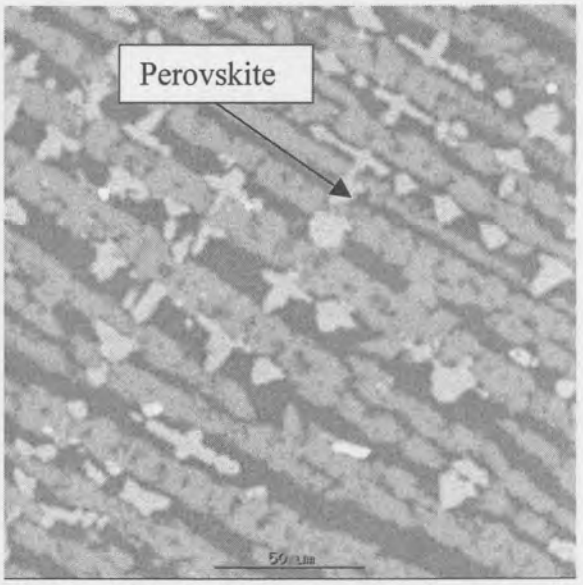

Figure 4.24: *SEM backscattered image of the mould flux of the austenitic steel with 10% Ti_3O_5*

In the SEM images of the mould flux for ferritic steel 2 phases have been identified: cuspidine as the light one and anorthite as the dark one.
In the case of the mould flux for the austenitic steel 2 main phases have been identified: cuspidine as the light one and nepheline as the dark. But a third phase can be seen for additions of all the titanium oxides TiO_2, Ti_2O_3 and Ti_3O_5.
This phase has been identified with EDX and XRD as perovskite.

An estimation of the precipitation temperature of perovskite has been performed using FactSage. That temperature has been found to be around 1160°C for 10 wt% TiO_2, 1240°C for 10 wt% Ti_2O_3 and 1220°C for 10 wt% Ti_3O_5. The volume fraction of perovskite precipitating above 1200°C for Ti_2O_3 and Ti_3O_5 are likely to small to have an effect on the viscosity (3.8 % for Ti_2O_3 and 2.7 % for Ti_3O_5 from FactSage calculation) and no departure from Arrhenius relationship is observed for all the three titanium oxides from 1400°C to 1200°C.

Referring to the change in basicity occuring for the mould flux of the austenitic steel and the precipitation of a solid phase rich in Ca, Ti and O in the molten slag during casting, viscosity measurements have also been done when increasing the basicity of this casting powder from 0.95 to 1.2 to match the basicity which arises during casting. This has been done by adding the required amount of CaO to the raw flux. The results are shown in the Figures 4.25 and 4.26 below for TiO_2 and Ti_2O_3 additions:

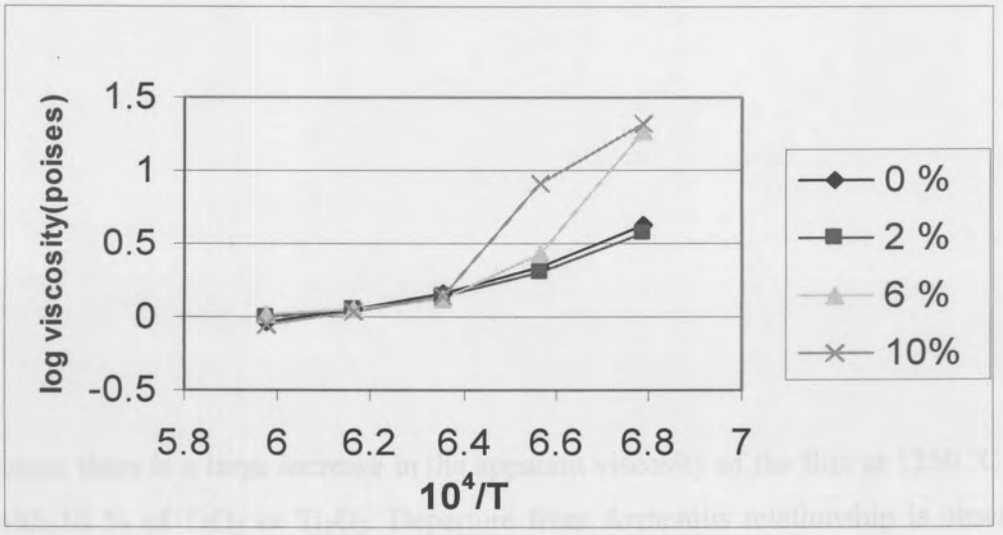

Figure 4.25: *Viscosity change of austenitic steel mould flux with temperature and TiO_2 content at* a *basicity of 1.2*

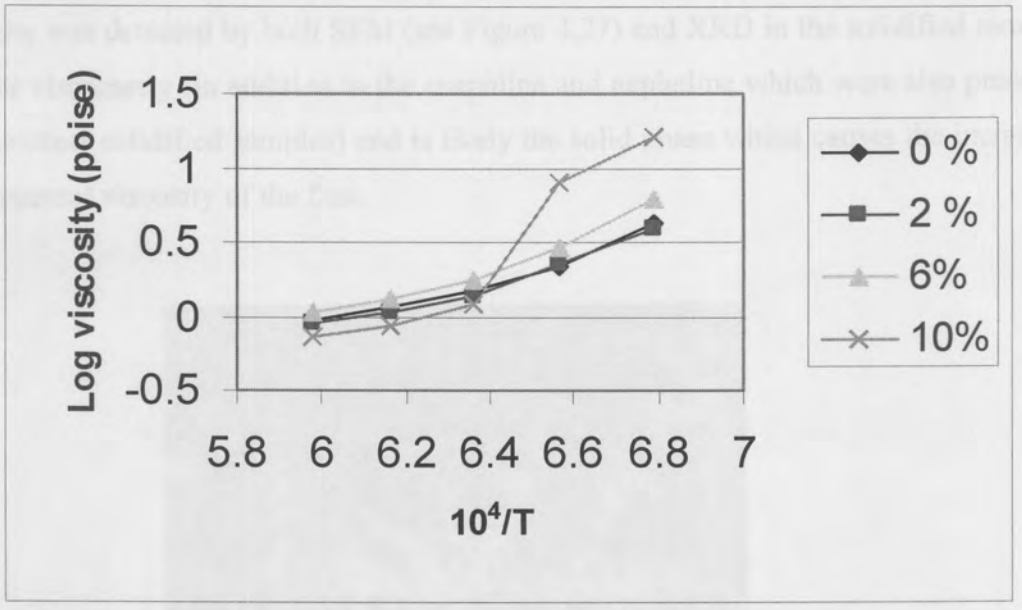

Figure 4.26: *Viscosity change of austenitic steel mould flux with temperature and Ti_2O_3 content at a basicity of 1.2*

In both cases there is a large increase in the apparent viscosity of the flux at 1250 °C and below with 10 % of TiO_2 or Ti_2O_3. Departure from Arrhenius relationship is observed from a temperature of 1250°C (that is, the graph of the logarithm of viscosity versus the reciprocal temperature is no longer a straight line). This indicates likely precipitation of solid particles in the flux.

Perovskite was detected by both SEM (see Figure 4.27) and XRD in the solidified mould flux after viscometry (in addition to the cuspidine and nepheline which were also present in all the other solidified samples) and is likely the solid phase which causes the increase in the apparent viscosity of the flux.

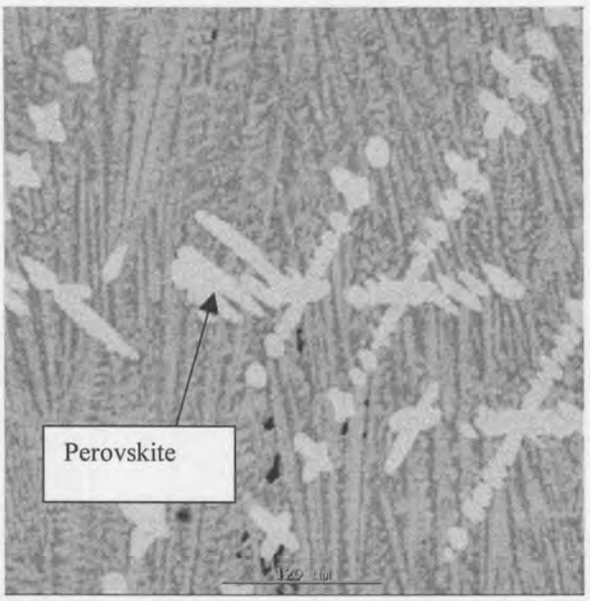

Figure 4.27: *SEM backscattered image of the mould flux for austenitic steel at a basicity of 1.2 with10 % of TiO_2 after viscosity measurements*

The presence of this solid material led to a non-Newtonian behaviour of the liquid flux. The Non-Newtonian behaviour of the liquid flux has been quantified.

A common method for characterising and quantifying non-Newtonian flow is to calculate the ratio of the fluid viscosity as measured at two different spindle speeds. In constructing the ratio, the viscosity value at the lower speed should be placed at the

numerator, the one at the higher speed as the denominator. These measurements are usually made at speeds that differ by a constant factor (for example, 2 and 10 RPM, 10 and 100 RPM, etc.). For pseudoplastic (shear-thinning) fluids, the ratio will be more than 1 as the degree of pseudoplasticity increases. Figure 4.28 shows this tendency for the casting powder for the austenitic stainless steel with a basicity of 1.2 with 10 % TiO_2 at temperatures below 1300 °C.

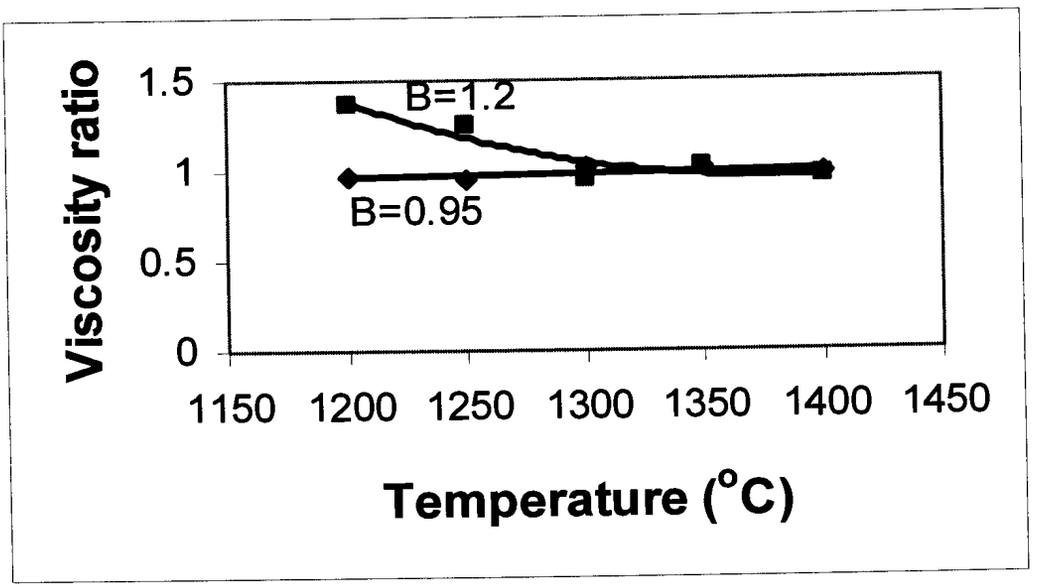

Figure 4.28: *Viscosity ratio for different temperatures for the mould flux of the austenitic steel at a basicity of 0.95 and a basicity of 1.2 with 10% TiO_2 and a ratio of rotation speeds of 2.*

Pseudoplastic fluids are non-Newtonian fluids which display a decreasing viscosity with an increasing shear rate or rotation speed. This can be seen in the Figures 4.29 below for the mould flux for austenitic steel at temperatures below 1250°C and below.

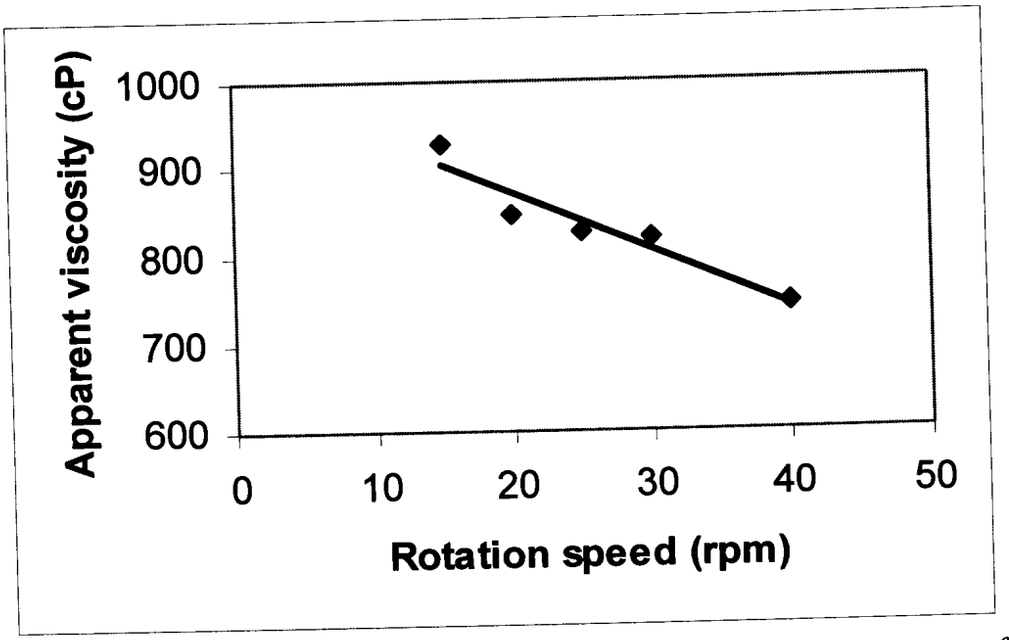

Figure 4.29: *Effect of rotation speed (shear rate) on the apparent viscosity of the mould flux of the austenitic steel at 1250°C with 10% TiO_2.*

One of the most commonly used relationship describing the viscosity of liquids containing solid suspensions is the Einstein-Roscoe type equations [Roscoe, 1952]:

$$\eta = \eta_o(1- af)^{-n}$$

Where η and η_o are the viscosity of the solid-containing and solid-free melt, respectively; f the fraction volume of solid particles in the melt; and a and n are constants. The reciprocal value of a represents the maximum amount of solid that could accommodate before the viscosity becomes "infinite". For spherical particles of a uniform size, Roscoe suggested a and n to be 1.35 and 2.5, respectively.

The fraction of solid f has been estimated from a FactSage calculation to be 7.7% at 1250°C and 10.6% at 1200°C for an addition of 10 wt% of TiO_2. The Einstein-Roscoe correlation hence predicts values of 286.8cP and 597.8cP. The measured values were respectively 828 cP and 2083cP.

The sharp increase in measured viscosity is much more than that predicted by Einstein - Roscoe equation, because probably the perovskite precipitate which is in dendritical form likely forms network instead of separate spherical particles.

The exact nature of perovskite precipitating has not been determined but is likely solid solution of $Ca_2Ti_2O_6$ and $Ca_2Ti_2O_5$ depending on whether the oxidation state of titanium oxides is maintained during the experiments. This was difficult to determine since the two perovskites have almost the same characterictics. The same effects have been noticed with both TiO_2 and Ti_2O_3. Departure from Arrhenius relationship has been observed at 1250°C in both cases for 10% TiOx and the amount of perovskite found from image analysis of the solidified samples after viscosity measurements was similar for 10 % TiO_2 (9.8%) and 10 % Ti_2O_3 (11.8%) additions.

Oxidation of Ti^{3+} toTi^{4+} needs very low oxygen potential. And it was not sure that those very low oxygen potentials were maintained during experiments with our set-up although the stainless steel crucible and the molybdenum spindle and its extension were not oxidised during experiments.

5. CONCLUSIONS

During continuous casting of Ti-stabilised stainless steels, there is a pick-up of Ti by the molten flux. In the case of a ferritic steel the TiO_2 content of the molten flux reached 3-4% and for the austenitic steel it reached 6 %.

The absorption of TiO_2 occurs mainly through the reaction of SiO_2 with TiN and Ti dissolved in the steel and hence increases the basicity of the powder.

Some spherical metallic particles have been observed in both cases and in the case of the austenitic steel solid precipitates of perovskite ($Ca_2Ti_2O_6$ or $Ca_2Ti_2O_5$) are formed. Perovskite is a high melting point compound (1970°C) and is formed above 1200°C when the basicity of the flux is above 1.1. This solid material is responsible for the increase of the apparent viscosity of the mould flux of the austenitic steel because the absorption of Ti by a slag is found to decrease the viscosity of casting powders when the basicity is below 1.

When the basicity of the powder is less than 1, TiO_2, Ti_2O_3 and Ti_3O_5 were found to decrease the viscosity of the powder.

The starting basicity of the casting powder is an important factor to be considered when casting Ti-stabilised stainless steels. It can be advised to have a starting basicity as low as to 0.7 so that precipitation of perovskite can be avoided and thus avoiding the increase of viscosity of the molten flux.

In the selection of casting powders, the crystallisation properties of the material to be used for continuous casting of titanium stabilised stainless steels must be compatible with the Ti and TiOx present in the steel, for example, a low crystallisation temperature is required with a moderate low viscosity. The flux must be able to absorb TiOx compounds without excessive increase in the crystallisation temperature. If the crystallisation temperature is increased excessively, lubrication in the mould suffers as the liquid film crystallises higher in the mould and the horizontal heat transfer between the solidified strand and the mould is significantly reduced. The horizontal heat transfer has a critical effect on process control and is important because certain serious problems in continuous casting are related to the magnitude of the heat transfer.

Thus, this study has to be continued with the effect of Ti oxides and metallic droplets on the crystallisation behaviour of the fluxes. This will lead to the effect of the titanium pick-up on the heat transfer between the solidified steel and the mould wall because titanium pickup during casting is expected to affect the heat transfer (TiO_2 being a well known nucleating agent for glasses).

6. REFERENCES

1. Barbieri L., Corradi A.B., Leonelli C., Siligardi C., Manfredini T. and Pellacani G.C., (1997), *Effect of TiO_2 addition on the properties of complex aluminosilicate glasses and glass ceramics*, Materials Research Bulletin, Vol. 32, No 6, 637-648.

2. Bezuidenhout G.A., (1999), *The effect of alumina pick-up on mould flux behaviour in continuous casting*, Master Thesis, University of Pretoria.

3. Bezuidenhout G.A., Pistorius P.C., (2000), *Effect of alumina pickup on mould flux viscosity in continuous slab casting*, Ironmaking and Steelmaking, Vol. 27, No.5, 387-391.

4. Bodsworth C. and Bell H.B., (1972), *Physical chemistry of iron and steel manufacture*, Second Edition, Longman Group Limited, London.

5. Bommaraju R., (1991), *Optimum selection and application of mold fluxes for carbon steels*, 1991 Steelmaking Conference Proceedings, 131-146.

6. Bourne M.C., (1982), *Food texture and viscosity: Concept and measurement*, Academic Press, Inc., New York.

7. Branion, R.V., (1987), *Mould fluxes for continuous casting & bottom pour teeming*, Iron and Steel Society, 3-13.

8. Brimacombe J.K, Samasekera I.V., (1979), *The thermal field in continuous casting moulds*, Canadian Metallurgical Quarterly, Vol.18, No3, 251-256.

9. Courtney L., Nuortie-Perkkio, Valaderes C.A.G, Richardson M.J and Mills K.C, (2000), *The crystallization of slag films formed in continuous casting*, Molten slags & Fluxes and Salts'2000 Conference. Published on CD-ROM.

10. Diehl S., Moore J.A. & Phillips R.J., (April 1995), *Improved spherical granule mold flux*, 78th Steelmaking Conference, Nashville, Tennesee, U.S.A.

11. The Japan Society for the Promotion of Science & the 19th Committee on Steelmaking, (1988), *Steelmaking Data Sourcebook,* Revised Edition, Gordon and Breach Science Publisher.

12. Johnston P.W., Brooks G., (1997), *Effect of Al_2O_3 and TiO_2 additions on the Lubrication characteristics of mould fluxes*, Molten Slags & Fluxes and Salts'97 Conference, 845-850.

13. Kanyakumari D., Paresh K.S., Shyam S.G. & Amit Chatterjee, (1993), *Effect of titania on the characteristics of blast furnace slags*, Steel Research, Vol. 64, No. 5, 232-239.

14. Kashiwaya Y., Cicutti C.E., Cramb A.W. & Ishi K., *Development of double and single Hot Thermocouple Technique for in situ observation and measurement of mold slag crystallisation,* ISIJ International, Vol. 38, No 4, 348 – 356.

15. Kawamoto M., Nakajima K.and Nakai K., (1994), *The melting rate of the mold powder for continuous casting*, Iron and Steel Society Transactions, Vol. 15, 123-128.

16. Kawamoto M., Kanazawa T., Hiraki S. and Kumakura S., (1997), *Mold flux for high speed continuous casting*, Molten Slags, Fluxes and Salts'97 Conference, 777-780.

17. Kim J. W., Choi J., Kwon O.D., Lee I.R., Shin Y.K. and Park J.S, (1992), *Viscous characteristics of synthetic mold powder for high speed continuous casting,* 4th International Conference on Molten Slags and Fluxes, Sendai, ISIJ, 468-473.

18. Kishi T., Takeuchi H., Yamamiya M., Tsuboi H., Nakano T., Ando T., (1987), *Mold powder technology for continuous casting of titanium-stabilised stainless steel*, Nippon Steel Technical Report No.34, 11-20.

19. Kromhout J.A, Van der Plas, (2000), *The melting speed of mould powders, determination and application in casting practice*, Molten Slags, Fluxes and salts Conference 2000, Published on CD-ROM.

20. Kyoden H., Diohara T. and Nomura O., (1987), *Development of mould powders for high speed continuous casting*, Mould Powders for Continuous Casting and Bottom Pour Teeming, Iron and Steel Society, 45-51.

21. Liao L. and. Fruehan R.J.,(1990), *Thermodynamics of Ti, Al and inclusion formation in stainless steel and nickel alloys*, Iron and Steel Society Transactions, vol.11, 105-111.

22. Mills KC, (1995), *Viscosity of molten slags [in:] Slags Atlas,* 2nd Edition, Verlag Stahleisen GmbH, 349-401.

23. Mills K.C., Courtney L., Fox A.B., Harris B., Idoyaga Z., Richardson M.J., (2002), *The use of thermal analysis in the determination of the crystalline fraction of slag films*, Thermochimica Acta 7058, 1-10.

24. Mills K.C., Franken M., Seethraman, Broadbent C. & Shiraishi Y., *Certification Report on Standard Reference Material (SRM) for High Temperature Viscosity Measurements*, NPL Report DMM(A) 147.

25. Muderscbach D., Drissen P. M., Kuhn M & Geilseler J., (2001), *Viscosity of slags,* Steel research 72, No3, 86-89.

26. Nakato H., Sakuraya T., Nozaki T., Emi T., (1987), *Physical and chemical Properties of casting powders affecting the mold lubrication during continuous casting*, Mould Powders for Continuous Casting & Bottom Pour Teeming, Iron and Steel Society, 23-29.

27. Nunnington R.C, Sutcliffe N., (2002), *The steelmaking and casting of Ti-stabilised stainless steel,* Iron and Steel Society /AIME, 59th Electric Furnace Conference and 19th Process Technology Conference Proceedings (U.S.A), 361-394.

28. Orban W., (2003), *Private Communication*, Columbus Stainless Steel.

29. Orrling C., Kashiwaya Y., Sridhar S. & Cramb A.W., (2000), *In Situ observation and thermal analysis of crystallization phenomenon in mold slags*, Molten Slags, Fluxes and Salts'2000, Published on CD-ROM.

30. Ozturk B., (1992), *Solubility of TiN in continuous casting powders*; communication to Metallurgical and Materials Transactions B, vol 23B, 523 – 526.

31. Ozturk B., Matway R. and Fruehan R.J.,(1995),*Thermodynamics of inclusion formation in Fe-Cr-Ti-N alloys*, Metallurgical and Materials Transactions B,vol.26B, 563-567.

32. Pehlke R.D., (1973), *Unit Processes of Extractive Metallurgy*, American Elsevier Publishing Company Inc.

33. Pelton, A.D., (2003), *Private communication,* Ecole Polytechnique de Montreal.

34. Quested P.N. & Monaghan B.J., (2000), *The measurement of thermophysical properties of molten slags and fluxes*, Molten slags, Fluxes and Salts'2000 Conference. Published on CD-ROM.

35. Riboud P.V., Larrecq M., (1979), *Lubrication and heat transfer in continuous casting mould*, Steelmaking Proceedings 1979, Vol.62, ISS-AIME, 54-62.

36. Riquier Y., Lambert V., Dumortier C.,(1997), *Mould's behavior during continuous casting of Ti-stabilised stainless steel*, Bulletin du Cercle d'Etudes des Metaux (France), Vol. 16, No. 14, 5.1 - 5.9.

37. Rocabois P., Pontoire J.N., Lehman J., Gaye H., (2000), *Crystallization kinetics of Al_2O_3-CaO-SiO_2 based oxide inclusions*, Molten Slags, Fluxes and Salts'2000 Conference. Published on CD-ROM.

38. Roscoe R., (1952), *The viscosity of suspensions of rigid spheres,* British Journal of Applied Physics, Vol. 3, 267-269.

39. Sakuraya T., Emi T., Emoto K. and Koshikawa T., (1982), *Development of mold fluxes for high-speed strand casting of slabs free from surface conditioning*, Second Iron and Steel Society/AIME, Process Technology Proceedings, 310-316.

40. Scheller P.R., (2002), *Redox reactions in slags during continuous Casting of stainless steel*, Proceedings of the Mills Symposium, Metals, Slags, Glasses: High Temperatures Properties & Phenomena, 487-493.

41. Schürmann E., Djurdjevic M., Ndeljkovic L., (1997), *Calculation of liquidus temperatures of low and high alloyed iron base melts from their chemical compositions by means of the equivalence factors,* Steel research, vol.68, 101-106.

42. Sharan, Jimbo I. and Cramb A.W.,(1995), *Fundamentals aspects of the casting of Titanium Treated Steels*, Iron and Steel Society Transactions, Vol.15, 95-99.

43. Sigworth G.K. and Elliot J.F., (1973), *The Thermodynamics of liquid dilute iron alloys*, Metal Science, Vol.8, 298 – 310.

44. Susa M., Mills K.C., Richardson R., Taylor R. and Steward D., (1994), *Thermal properties of slag films taken from continuous casting mould*, Ironmaking and Steelmaking, Vol.21, No.4, 279-286.

45. Thomas B.G, Stone D.T, (1999), *Measurement and modeling of heat transfer across interfacial mold flux layers*, Canadian Metallurgical Quarterly, Vol. 38, No 5, 363-375.

46. Turkdogan E.T., (1983), *Physical properties of molten slags and glasses*, The Metals Society, London.

47. Turkdogan E.T.,(1990), *Causes and effect of nitride and carbonitride precipitation during continuous casting*, Iron and Steel Society Transactions, vol.11, 39-53.

Appendix 1 Bob and Apparatus constant for viscosity calculation

1. Crucible and Bob used for viscosity measurements

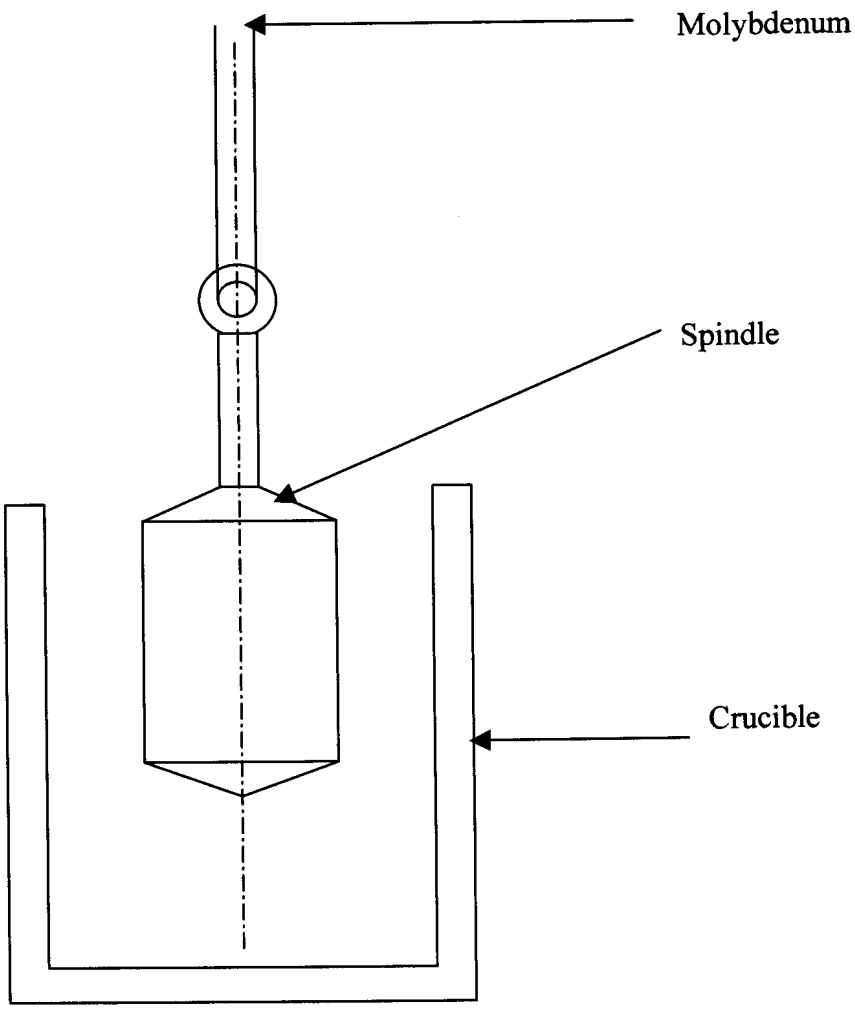

2. Apparatus constant for viscosity calculations

Speed (rpm)	10	15	20	25	30	40	60	80	100	120	140
$\frac{1}{G}$	44.6	30.0	22.0	17.8	14.5	10.7	8.0	5.8	4.4	3.5	3.1

$\eta = D^* (\frac{1}{G})$ where η = viscosity

D = scale deflection of the viscometer
G = apparatus constant

Appendix 2 EDX Analysis of sampled fluxes during casting for mould flux for autenitic steel 321

Heat 1

	Casting time (min)					
	0	11	20	29	38	47
CaO	36.2	37.8	36.15	37.7	37.3	37.5
SiO_2	38	33.7	32.2	31.7	31.96	32.06
Al_2O_3	6.3	6.2	5.8	6.9	5.8	5.9
Na_2O	7.8	7.1	6.3	6.6	6	6.2
TiO_2	0	3.68	5.79	5.45	6	5.77
MgO	0.7	0.4	0.3	0.3	0.4	0.4
K_2O	0.2	0.3	0.2	0.3	0.3	0.2
MnO	0	1.5	1.3	1.4	1.4	1.5
F	7.6	8.5	8.9	8	7.2	8.2
Cr_2O_3	0	1.1	0.88	1.2	1.2	1.1
Fe_2O_3	1.1	0.5	0.6	0.3	0.5	0.6

Heat 2

	Casting time (min)					
	0	10	19	27	35	43
CaO	36.2	38.2	39.1	40.2	39.5	38.4
SiO_2	38	34.1	31.8	31.4	31.6	31.2
Al_2O_3	6.3	6.2	5.8	6.1	5.6	6.5
Na_2O	7.8	7.5	7.6	6.8	7.2	7.3
TiO_2	0	5	5.7	5.6	5.9	5.8
MgO	0.7	0.4	0.4	0.4	0.4	0.4
K_2O	0.4	0.3	0.2	0.2	0.2	0.2
MnO	0	1.3	1.4	1.4	1.8	1.6
F	7.6	6.2	8.2	7.5	8.3	7.8
Cr_2O_3	0	0.8	0.8	0.9	1	1.1
Fe_2O_3	1.1	0.1	0	0.5	0.2	0

2. EDX analysis for sampled flux during casting of ferritic steel 409

Heat 1

	Casting time (min)					
	0	5	13	23	33	42
CaO	30.2	32.2	31.3	32.1	30.5	31.6
SiO_2	37	35.8	35.3	34.9	34.9	35
Al_2O_3	6.3	6.2	5.8	6.9	5.8	5.9
Na_2O	10.9	9.9	8.6	7.8	8.9	9.1
TiO_2	0.186	1.5	2.5	3.1	3.3	3.2
MgO	1.1	0.8	1.2	1.1	0.8	1.1
K_2O	0.507	0.3	0.4	0.3	0.3	0.3
MnO	0.073	1.3	1.4	1.4	1.2	1.5
F	6.06	7.8	8.2	7.8	7.2	9.5
Cr_2O_3	0	1.5	1.4	1.2	1.2	1.1
Fe_2O_3	1.89	0.71	1.2	0.82	0.85	1.1

Heat 2

	Casting time (min)					
	0	4	14	24	34	44
CaO	30.2	29.3	29.6	30.8	28.2	31.2
SiO_2	37	35.1	34.7	34.3	34.1	34.3
Al_2O_3	6.3	5.7	6.7	5.9	6.2	7
Na_2O	10.9	8.5	10.2	8.9	7.8	9.2
TiO_2	0.186	2.8	3.4	4.25	4.15	4.1
MgO	1.1	1.3	0.9	0.9	1	1.1
K_2O	0.507	0.5	0.3	0.4	0.5	0.3
MnO	0.073	1.2	1.1	0.9	1	0.9
F	6.06	8.1	7.8	6.2	8.5	7.5
Cr_2O_3	0	1.1	0.9	1.3	1.1	0.8
Fe_2O_3	1.89	1.1	0.9	1.2	0.85	1

Appendix 3 Viscosity results

A.Viscosity results (cP) for the mould flux of the ferritic steel

1. TiO_2 effect

	1400°C	1350°C	1300°C	1250°C	1200°C
0%	173.06	234.82	325.85	485.36	675.2
2%	174.5	229.68	319.66	465.66	661.2
6%	173	218	286	410	591
10%	146	185	249	349	507

2. Ti_2O_3 effect

	1400°C	1350°C	1300°C	1250°C	1200°C
0%	173.06	234.82	325.85	485.36	675.2
2%	172.1	228.3	318.9	462.4	658.2
6%	185	235	325	443	583
10%	166	199	263	363	551

3. Ti_3O_5 effect

	1400°C	1350°C	1300°C	1250°C	1200°C
0%	173.06	234.82	325.85	485.36	675.2
2%	176.2	225.1	327.5	470.3	665.2
6%	173.87	220.02	320.3	465.12	670.22
10%	165.1	210.6	287.1	416.5	602.1

B. Viscosity results for the mould flux of the austenitic steel (cP) at a basicity of 0.95

1. TiO_2 effect

	1400°C	1350°C	1300°C	1250°C	1200°C
0%	111.3	149.4	214.5	310.1	430.6
2%	105.2	142.3	198.5	282.3	398.2
6%	97.2	127.3	181.2	255.3	356.2
8%	83.2	107.8	140.2	188.9	260.4
10%	72.2	90.7	120.2	163.8	235.3

2. Ti_2O_3 effect

	1400°C	1350°C	1300°C	1250°C	1200°C
0%	111.3	149.4	214.5	310.1	430.6
2%	103.3	137.7	196.3	280.3	388.5
6%	88.5	122.3	169.5	228.6	322.3
10%	84.5	116.3	152.6	218.3	315.2

3. Ti_3O_5 effect

	1400°C	1350°C	1300°C	1250°C	1200°C
0%	111.3	149.4	214.5	310.1	430.6
2%	102.2	135.3	196.3	281.1	387.3
6%	98.3	130.2	187.2	260.2	376.2
10%	88.5	116.3	160.2	220.4	317.2

C. Viscosity results for the mould flux of the austenitic steel (cP) at a basicity of 1.2

1. TiO_2 effect

	1400°C	1350°C	1300°C	1250°C	1200°C
0%	92.1	114.2	147.7	218.2	416.2
2%	98.12	112.2	138.4	204.3	380.6
6%	102.2	115.2	135.6	270.5	1850.2
10%	88.3	109.2	140.6	828.4	2083.2

2. Ti_2O_3 effect

	1400°C	1350°C	1300°C	1250°C	1200°C
0%	92.1	114.2	147.7	218.2	416.2
2%	88.6	106.2	136.4	222.3	386.6
6%	108.3	128.7	177.7	293.7	617.3
10%	72.6	85.8	118.3	808.1	1652.32